

DETECTING THE SHORLINE CHANGE OF QARUH ISLAND, KUWAIT, USING
REMOTE SENSING AND GIS

by

Faisal Anzah, B.A.

A thesis submitted to the Graduate Council of
Texas State University in partial fulfillment
of the requirements for the degree of
Master of Science
with a Major in Geography
May 2016

Committee Members:

David R. Butler, Chair

Richard Dixon

Nathan Currit

COPYRIGHT

by

Faisal Anzah

2016

FAIR USE AND AUTHOR'S PERMISSION STATEMENT

Fair Use

This work is protected by the Copyright Laws of the United States (Public Law 94-553, section 107). Consistent with fair use as defined in the Copyright Laws, brief quotations from this material are allowed with proper acknowledgment. Use of this material for financial gain without the author's express written permission is not allowed.

Duplication Permission

As the copyright holder of this work I, Faisal Anzah, authorize duplication of this work, in whole or in part, for educational or scholarly purposes only.

DEDICATION

I would like to dedicate this thesis to my parents, who have taught me how to be self-reliant and who fostered a sense of persistence and ambition in me. This thesis is also dedicated to my wife and my two sons, who have supported me by travelling with me and being with me for every second of my journey through my master's degree.

ACKNOWLEDGEMENTS

First of all, I would like to thank God for giving me help and assistance in all the challenges that I have faced. Second, I would like to thank my advisor, Dr. Butler, who has supported me with his academic skill and knowledge. Without his guidance, this thesis would not have been accomplished. In addition, I would like to thank Dr. Dixon and Dr. Currit for their important advice.

Third, I would also like to thank Allison for her frequent and generous help. Furthermore, I owe many thanks to the Senyar Diving Team, who provided me with the opportunity to visit Qaruh Island to do my fieldwork, and to Dr. Mohamad Alkhalidi, who provided me with important figures. Lastly, I would like to thank my close friend Abdullatif for volunteering to help me with my fieldwork trip.

TABLE OF CONTENTS

	Page
ACKNOWLEDGEMENTS	v
LIST OF TABLES	viii
LIST OF FIGURES	ix
CHAPTER	
I. INTRODUCTION	1
Research Background	2
Conceptual Framework	4
II. LITERATURE REVIEW	6
The Nature of Shoreline Change	6
Wind-Driven Waves, Littoral Drift, Tides, and Anthropogenic Activities	6
Anthropogenic Factors	8
The Environmental Role of Coral Reef along Shorelines	9
The Structure of Coral Reef	9
Types of Coral Reef	9
Coral Reef Zonation	10
Ecological and Geomorphological Benefits of Fringing Coral Reefs	11
Coral Reef Disturbance	12
Shoreline Mapping Techniques	14
Using Remote Sensing and GIS in Shoreline Change Detection: Methodological Considerations	16
Spatial and Spectral Resolution of Satellite Images	16
Geometric Correction	17

Shoreline Indicators.....	17
Delineation of the Shoreline Indicator	19
Rate of Change Statistics.....	20
III. RESEARCH METHODS.....	22
Site and Situation.....	22
Physical Conditions	22
Datasets.....	26
Analysis	26
Geometric Correction of Satellite Images	26
Shoreline Extraction and Calculation of Uncertainty.....	27
Rate of Change Calculation.....	28
Fieldwork.....	30
IV. RESULTS	31
Shoreline Change from 2009 to 2013	31
Shoreline Change from 2013 to 2015	33
Shoreline Change from 2009 to 2015	35
Fieldwork Result: Shoreline Change Verification	38
V. DISCUSSION	42
VI. CONCLUSION.....	48
REFERENCES	51

LIST OF TABLES

Table	Page
1. List of Statistical Approaches Provided by DSAS and Their Associated Definitions	21
2. Value of Errors and Uncertainty Associated with Each Shoreline	29

LIST OF FIGURES

Figure	Page
1. Conceptual Framework of Shoreline Change in Qaruh Island, Kuwait.	5
2. Map of the Study Area.....	25
3. Map Showing the Extracted Shorelines, Baselines, and Transect Lines.	29
4. Map Showing the Result of the End of Point Method, 2009–2013	32
5. Map Showing the Result of the Net Shoreline Movement Method, 2009–2013.....	32
6. Map Showing the Result of the End of Point Method, 2013–2015	34
7. Map Showing the Result of the Net Shoreline Movement Method, 2013–2015.....	34
8. Map Showing the Result of the End of Point Method, 2009–2015	36
9. Map Showing the Result of the Net Shoreline Movement Method, 2009–2015.....	36
10. Map Showing the Result of the Linear Regression Method, 2009–2015	37
11. Map Showing the Result of the Weighted Linear Regression Method, 2009–2015 ..	37
12. Photo Showing the Wave-Cut Platform in the Southeast Part of the Island.....	39
13. Photo Showing the Seawall in the Northwest Part of the Island	39
14. Photo Showing Beach Ridges in Accretion Areas.....	40
15. Photo Showing Small Sand Dune Underneath the Jetty and Beach Ridges in the Southwest Part of the Island.....	40
16. Photo Showing Cusps in the No Change Area	41
17. Wind Rose around Qaruh Island.....	44
18. Wave Rose around Qaruh Island	45

19. Nautical Chart of the Arabian Gulf with Red Circle Showing Qaruh's Location	45
20. Bathymetry Map of the Arabian Gulf.....	46
21. Satellite Image of the Study Areas Showing the Location of Boats on the Island	46
22. Aerial Photo of the Island Showing How Closely the East Part Is Fringed by the Reef	47

I. INTRODUCTION

Shoreline is defined as the edge that separates land and water (Pajak and Leatherman 2002). There are more than 347,984 km of shoreline in the world. Over 60 percent of the world's population is geographically located within 100 km of the coastal areas (Vitousek et al. 1997). The shape and location of shorelines dynamically change over time. Coastal processes such as wind-generated waves, longshore drift and tides influence shorelines. Anthropogenic activities also have a great influence on the change of shorelines (Morton 1977). These factors are affecting shorelines all over the world. Coral islands are ecologically important because they support a high rate of biodiversity, but these coral islands are experiencing environmental problems because of shoreline change; hence, any threat that affects their shorelines will also affect their biodiversity role. Scientists have spent enormous amounts of time trying to understand this problem and have come up with an approach to understanding the behavior of shoreline change which is called shoreline mapping. Shoreline mapping has been assisting coastal scientists who manage coastal zones and determine legal boundaries (Sukcharoenpong 2014). According to Morton (1979), global scientific and coastal management objectives should be driven by shoreline mapping and future prediction of shorelines' positions. Over the past few decades, scientists have established several methods to map shorelines, including ground survey methods, aerial photos, GPS surveys, satellite images, and light detection and ranging (LIDAR). They have used these methods to detect shorelines change based on temporal scales, quantifying either long-term or short-term shoreline change. Long-term shoreline change ranges from decades to centuries, whereas short-term shoreline change ranges from seasons to a few years (Arias Moran 2003).

Qaruh Island is a coral island that belongs to the state of Kuwait. The island is considered to be the most diverse and attractive coral reef ecosystem in Kuwait (Carpenter et al. 1997). It is undoubtedly a spectacular marine natural resource of Kuwait which hosts many marine species that live on the island, such as coral fishes and turtles (Carpenter et al. 1997). However, the shoreline of the island is experiencing tremendous change, which is threatening its ecological riches. Thus, this thesis project seeks to utilize high-resolution satellite images obtained via remote sensing and a geographic information system (GIS) to gain a better understanding of the morphological behavior (erosion and accretion) of Qaruh Island over a short-term period (2009–2015).

Research Background

Qaruh Island is a reef island made of coral reef deposits. The name Qaruh stems from the presence of petroleum sediments, or *qar* (tar) in the local language, which seeped from its coast and was distributed by the action of waves (Al-Kandari 2007). Ecologically, reef islands can serve as a habitat for marine species and they also serve as a tourism attraction. Due to their ecological and tourism importance, reef islands are subject to natural and anthropogenic processes. Natural processes include erosion and sedimentation, while anthropogenic activities include, diving, fishing, and coastal construction such as ports and resorts.

Qaruh Island is a reef island wilderness with abundant wildlife. Qaruh Island is considered to be the most diverse and attractive coral reef ecosystem in Kuwait (Carpenter et al. 1997). It is undoubtedly a very spectacular marine natural resource of Kuwait (Carpenter et al. 1997). It hosts many marine species that live on the island, such as coral fishes and turtles (Carpenter et al. 1997). According to Carpenter et al. (1997),

127 species have been recorded at the Kuwaiti coral islands (Qaruh and Kobbar). Qaruh Island is also a nesting spot for two endangered turtle species, the green turtle (*Chelonia mydas*) and the hawksbill turtle (*Eretmochelys imbricata*) (Morgan 1988). Beside these environmental benefits, Qaruh Island is the farthest island from the Kuwaiti coastline, and thus it is the first line of coastal defense.

Qaruh Island is experiencing a serious environmental problem: it is threatened with disappearance due to a high rate of erosion (Alsulaimani 2013). Only two studies have sought to investigate this problem, that of Al-Kandari (2007) and that of Neelamani et al. (2007). Al-Kandari (2007) studied the island's shoreline using a module-based shoreline change analysis. The module consisted of two steps. The first step was transforming the offshore waves to the nearshore using the STWAVE model. The STWAVE model depends on a variety of inputs such as wave conditions and bathymetric data. The wave condition data were based on 12 years of hindcast data from a location southeast of the island. The bathymetric data were obtained from a survey performed around the island and from NOAA. Prior to 2006, the global bathymetric data collected by NOAA were at a 3.7-km-grid size (NOAA 2006), which is a very coarse resolution. The second step of Al-Kandari's model was calculating the net and gross sediment transport using a simple wave transformation model. This was done using the output from the first step as input in a simple wave transformation model in order to determine the breaker wave conditions. Al-Kandari's final results showed that the island was exposed to high erosion in the northwestern section and low erosion in the south section, and that the northeastern and the southwestern sections were accretion areas.

Neelamani et al. (2007) conducted another study to investigate the problem. The study used an image-based shoreline change analysis. Comparison between 1989 and 2003 LADSAT images was used to uncover the trend of the shoreline change. The study results were completely the opposite of those obtained by Al-Kandari (2007). Neelamani et al.'s results showed that accretion was taking place in the southwest to northwest sections and the west section, but that erosion was taking place in the north and southeast sections. Moreover, Neelamani et al. (2007) found no change in a small portion of the northwest and northeast sections.

Conceptual Framework

The diagram in Figure 1 illustrates the conceptual responsible factors that are hypothesized to be involved in changing the shoreline of Qaruh Island directly and indirectly. Certain coastal processes (wind-generated waves, longshore drift, and tides) and anthropogenic and biological activities affect the shoreline directly. The fringing reef that buffers the shoreline of the island plays an important role in mitigating the effects of these factors; in other words, it serves as a biological barrier (bioprotection). These factors may also affect the shoreline indirectly by affecting and deteriorating the status of the fringing reef that buffers the shoreline of the island such that the fringing reef can no longer protect the shoreline effectively.

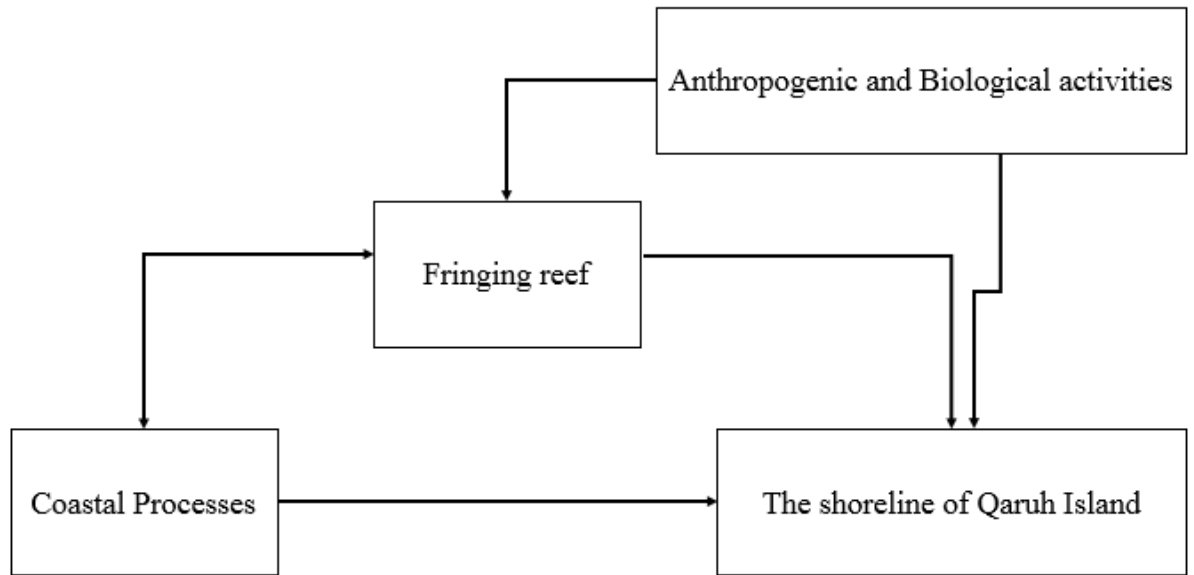


Figure 1. Conceptual Framework of Shoreline Change in Qaruh Island, Kuwait.

II. LITERATURE REVIEW

The Nature of Shoreline Change

Shoreline is the edge between land and water (Dolan et al. 1980). This definition seems simple; however, practically it is very hard to separate land from water because the position of the shoreline is continually changing (Boak and Turner 2005). Many factors contribute to this change: waves, longshore drift, tides, and anthropogenic activities.

Wind-Driven Waves, Littoral Drift, Tides, and Anthropogenic Activities

The vertical displacement of the surface of water that results from the transfer of energy from winds to the water surface is known as wind-driven waves (Davidson-Arnott 2010). When waves approach the coastline, they release their energy (Keller and DeVecchio 2011). Fetch is the surface distance of the ocean that winds blow over (Keller and DeVecchio 2011). The greater the wind speed, blowing duration, and the fetch, the larger the waves and the larger the erosion (Short 2012). On the other hand, when the waves slow down, (low-energy) deposition occurs. The size of sediment controls the deposition processes: deposition occurs for large sediments such as gravels and boulders, and fine sediments such as silt and clay remain suspended (Davidson-Arnott 2010). Moreover, as the waves break on the shore, there are two types of waves, constructive waves and destructive waves. Constructive waves occur when the swash is bigger than the backwash (Pask, Tieh, and Pask 2007). As a result, sediments are carried onto the beach (deposition). Conversely, destructive waves occur when the backwash is greater than the swash (Pask, Tieh, and Pask 2007). Because of destructive waves, sediment is carried away from the land (erosion). This process is called beach drift, and it is the first step of a process called littoral transport (Keller and DeVecchio 2011). Wave action is

responsible for the creation of erosional features such as cliffs, wave-cut platforms, sea stacks, and sea tunnels, and many other features (Huggett 2011). This process depends on three factors: wave energy, the resistance of the shore materials, and the slope degree of the shore (Huggett 2011). Sea cliffs, sea stacks, and sea tunnels are associated with rocky and steep beaches, whereas wave-cut platforms are associated with sandy and gentle slopes or horizontal beaches (Huggett 2011). Waves can also create a depositional feature called beach ridges, defined as the stacked up or accumulated sand or shingle which occurs as a result of wave action along a prograding beach (Huggett 2011).

Another type of littoral transport is the longshore drift (Keller and DeVecchio 2011), which occurs when waves reach the shore at an angle: the swash carries the sediment in the ocean to the shore at an oblique angle, while the backwash carries the sediment at a right angle down the shore because of the effect of gravity (Pask, Tieh, and Pask 2007). The direction of the waves, which is affected by the direction of the wind, affects the direction of the longshore drift (Pask, Tieh, and Pask 2007). Longshore drift is responsible for the creation of depositional features such as spits, forelands, and many other features (Huggett 2011). Depositional landforms may be simply categorized by their degree of attachment to the beach (Huggett 2011). Depositional landforms connected to the beach at one end are spits and forelands (Huggett 2011). Depositional features such as spits and forelands and many other features occur when the longshore drift faces an obstacle or the water energy decreases (Huggett 2011). Spits and forelands are similar, but the length of spits is greater than the width, whereas forelands have a width greater than their length (Huggett 2011). Looped barriers, tombolos, and barrier

beaches are depositional features that are connected to the beach at two ends, and barrier islands are disconnected from land (Huggett 2011).

Tides are defined as the cyclic rise and fall of the ocean. Because of small differences in gravitational effects between the Earth, Sun, and Moon in spatial relationship with positions on the surface of the Earth, tides occur (Short 2012). The fluctuation of tides is significant because it controls the vertical distance over which waves and currents are effective in changing shorelines, and combined with the slope of a shoreline, tidal range defines the extent of the intertidal zone, which is the area between high and low tide (Summerfield 2014). For instance, high tides combined with strong winds can push the sea water level up, thereby exposing dunes and beach to heavy attack by incoming waves and causing erosion, especially on sandy beaches. Coastal erosion also occurs mostly during high tides, leading to shoreline retreat as well as loss of land. All in all, high tides will result in erosion, while low tides may result in accretion (Houston 2015). (For more details about coastal processes and landforms, see Davidson-Arnott 2010; Huggett 2011).

Anthropogenic Factors

Anthropogenic factors also cause changes in the position and shape of the shoreline, especially because human activities cause erosion, and may alter the sediment transport processes (Reusser, Bierman, and Rood 2015). Beach nourishment and dredged sand disposed along inlets have both contributed to the changing Florida shoreline over time (Houston and Dean 2014). Human activities affect the availability of the sediment that sustains beaches, increasing the risk of soil erosion along the shoreline (Morton 1979). A notable example that illustrates the impact of human activities on a coastal

environment is the case of Folly Island in South Carolina. In 1986, a 3-km long rock jetty was built to shelter the entrance of Charleston Harbor, and the jetty partially obstructed the delivery of sediment by coastal currents and caused severe shoreline erosion on the island (Keller and Devecchio 2011).

The Environmental Role of Coral Reef along Shorelines

The Structure of Coral Reef

Coral reefs are restricted to areas with shallow water, light intensity, and clear and salty water (Galko 2002). Calcium carbonate is the main component of coral reefs. The calcium carbonate is absorbed from the surrounding water by coral polyps and each polyp excretes a skeleton of limestone, which is attached to seabed rocks or to the dead skeletons (Galko 2002). Thus, the size of coral reefs varies according to the availability of the polyps; the greater the number of the polyps, the greater the structure's size is. The growth rate is also affected by the water temperature. In cold waters, the growth rate is mostly slower than the growth rate in warmer areas (Spalding, Ravilious, and Green 2001). Other environmental factors, such as disease, sedimentation, sunlight, rising temperatures, and the salinity of the water, also affect the growth rate of coral reefs (Spalding, Ravilious, and Green 2001).

Types of Coral Reef

Fringing reef is found mostly along the shoreline. This type of coral reef has a shallow back reef or none at all, a fact that distinguishes it from the other major coral reefs (Darwin and Bonney 1897; Spalding, Ravilious, and Green 2001; Karleskint, Turner, and Small 2012). Fringing reef is the most common type and it is believed to be

the first one to exist on a landmass (Goldberg 2013). Barrier reef is the other common type of coral reef; it is very similar to the fringing reef except that it is found further away from the shore (Darwin and Bonney 1897; Spalding, Ravilious, and Green 2001; Karleskint, Turner, and Small 2012). In addition, some of the portions of the barrier reef are deep (Darwin and Bonney 1897). Atoll reef is the other main type of coral. This type has a ring-like shape, and it surrounds a lagoon partially or entirely (Darwin and Bonney 1897; Spalding, Ravilious, and Green 2001; Karleskint, Turner, and Small 2012).

Coral Reef Zonation

The location or zone where a coral reef exists is determined by factors such as light, wave energy, depth, and sedimentation (Tunnell et al. 2007). In areas closest to the shore there is the back reef or the reef flat. The zones are shallow, extending to the reef crest (Spalding, Ravilious, and Green 2001). These sediments will cover the coral reef and block the sunlight. The width of the reef flats ranges from a few meters to kilometers, while the depth ranges from a few centimeters to several meters (Block [2007]). The primary factors that inhibit the survival of coral reefs in this zone are a reef's exposure when the tides are not high, whereas it is sheltered by other zones from wave action. Thus, sediment resulting from wave erosion limits the coral reef growth in this zone (Tunnell et al. 2007). In spite of the fact that living corals are limited to the seaward area of this zone, enormous numbers of creatures such as mollusks, worms, and decapod crustaceans are supported by its microhabitats (Barnes 1987; Lalli and Parsons 1995; Sumich 1996). A distance from the shoreline is the alga ridge or reef crest that separates the reef flat from the fore reef. It forms the highest part of the reef, but the environment is not very conducive due to exposure to high waves (Block [2007]). This zone is also

called the algal ridge because it hosts various types of algae, such as calcareous red algae (Barnes 1987; Lalli and Parsons 1995; Sumich, 1996; Block [2007]).

The fore reef is the other zone where coral reefs exist, and it is the farthest zone from the shore. This zone is affected by limited wave action because it falls sharply toward the seabed, which makes it habitable for a large number of organisms (Spalding, Ravilious, and Green 2001). However, because coral reefs are dependent on light and temperature, and the deeper the reef the lower the levels of light and temperature, the biological conditions of this zone change rapidly with the depth and exposure (Karlson 2002). Consequently, high diversity is found at shallower depths.

Ecological and Geomorphological Benefits of Fringing Coral Reefs

The fringing coral reef can be said to have an ecological benefit to the economy since it enables the survival of these marine animals, thus providing seafood such as crustaceans and fish (Moberg and Folke 1999). The seaweed found in the reef is known to aid the pharmaceutical industry in the manufacture of anti-inflammatory, anticancer, antimicrobial, and HIV drugs (Carté 1996; Moberg and Folke 1999; Sorokin 2013). The skeletons of reef structure are also important in monitoring the level of pollution in the environment over a particular period of time (Dodge and Gilbert 1984; Howard and Brown 1984).

The location of the fringing coral reefs along the shoreline has a geomorphic benefit of protecting the shore from erosion. This geomorphic benefit is known as bioprotection (Naylor, Viles, and Carter 2002; Naylor and Viles 2002). The presence of reefs along the shoreline ensures that there is no excessive erosion that would affect shorelines. The coral reefs dissipate wave energy, thus enabling the growth of grass,

which in turn protects the shoreline from erosion (Spalding, Ravilious, and Green 2001). The mangrove ecosystem may also exist as a result of the reduction of wave energy due to coral reefs (Moberg and Folke 1999), and this ecosystem further protects the shoreline. The coral reefs are able to build up a land mass buffer that enables various plants to grow, thus protecting the shoreline. This buffering ability makes the reefs capable of protecting the shoreline and human lives as well. The status of the coral reefs depends on the activities that are carried out along the coast (Spalding, Ravilious, and Green 2001). Activities that are harmful to the coral reefs also affect the shoreline indirectly. For example, a coral reef might be disturbed by the unusual down-drifted sediment load produced from mangrove swamp erosion that is caused by deforestation, which limits the reef's ability to act as a buffer against the strong waves and storms (Goudie and Viles 2013). It is therefore evident that fringing coral reefs should be protected in all ways possible due to their ecological and geomorphological benefits.

Coral Reef Disturbance

Despite the ecological and geomorphic benefits that coral reefs have, there are various natural threats that endanger their existence and their bioprotective role. The worst thing about these causes is that they are natural, and thus, very limited efforts can be undertaken to mitigate them (Dimitrov 2006). For instance, coral reef destruction will occur when strong waves associated with hurricane winds interfere with the coral reefs (Karleskint, Turner, and Small 2012; Spalding, Ravilious, and Green 2001). Coral bleaching resulting from increased water temperature also destroys coral reefs (Nyström, Folke, and Moberg 2000; Spalding, Ravilious, and Green 2001; Karleskint, Turner, and Small 2012). Other natural occurrences that threaten coral reefs include volcanic

activities and earthquakes (Nyström, Folke, and Moberg 2000). Beside natural forces (waves, longdrift, tides), organisms such as plants and animals are also considered to be geomorphic agents. According to Butler (1995), the geomorphic processes that result from animal activities are known as zoogeomorphic factors or processes, of which bioerosion is one. Neumann (1966, 92) defined bioerosion as the “destruction and removal of consolidated mineral or lithic substrate by the direct action of organisms”. Bioerosion occurs in ocean substrates as opposed to terrestrial ones and is caused by marine creatures such as fish, sponges, crustaceans, and echinoids (Hutchings 2010). The coral reefs accumulate calcium carbonate compounds on their skeletons, but bioeroder organisms break this carbonate into sand and rubble (Goldberg 2013). Fish cause bioerosion either by eating the algae found in the living coral reefs or eating dead coral reefs (Spalding, Ravilious, and Green 2001). One type of fish that is known to cause massive bioerosion is the parrotfish. Beside their erosional role, parrotfish also transport the material that they excavated to another spot within the reef system (Bellwood 1995). Sponges also cause bioerosion by chemically dissolving the carbonate skeletons, which causes them to be easily broken (Spalding, Ravilious, and Green 2001). Therefore, bioerosion reduces the bioprotective role of the coral reef against the incoming waves.

Coral reefs are also exposed to anthropogenic disturbance brought about by human activities. Pollution is a major anthropogenic threat. The main type of pollution that affects marine life such as coral reefs is the water pollution. Water pollution is a result of poor sewage treatment, nutrient enrichment that results from human waste, and agricultural runoff (Spalding, Ravilious, and Green 2001; Karleskint, Turner, and Small 2012). The increase in nutrients will result in increasing the bioerosion rate (Hallock

1988). Overfishing also affects the coral reef ecosystem in indirect ways (Nyström, Folke, and Moberg 2000). Decreasing the fish biomass will increase the sea urchin population, and that will increase the bioerosion rate (Nyström, Folke, and Moberg 2000). It is therefore crucial to control human activities that affect the status of coral reefs—activities such as deep sea fishing, water pollution or coastal development. The natural threats may not be easy to control, but the anthropogenic ones can easily be contained. The geomorphic and ecological benefits reaped from the coral reefs should provide motivation enough for the control of such human activities.

Shoreline Mapping Techniques

Scientists have developed a variety of methods to map shorelines. In the past, scientists mapped shorelines using ground survey methods (Liu 2009). This was done by using a plane table and a rod to measure the direction and distance of the shoreline (Smith 1981; Graham, Sault, and Bailey 2003; Liu 2009). In the 1920s, aerial photos replaced the traditional method (Smith 1981; Graham, Sault, and Bailey 2003; Liu 2009). Aerial photos are made by cameras attached to aircraft; a comparison of images over time then reveals shoreline changes. The GPS gives aerial images that are spatially referenced to ensure that users can get accurate information on the location of shorelines (NOAA 2014). However, the spatial resolution of the aerial photos depends on the altitude of the platform (Neteler and Mitasova 2002; Kato 2008). For instance, high-resolution aerial photos are taken from low-altitude platforms (Kato 2008). Aerial photos are the most common data used in shoreline change detection, but their use depends on their availability (Boak and Turner 2005).

GPS survey is another shoreline mapping technique, and one whose use is increasing. Kinematic differential GPS on top of a four-wheel-drive vehicle is another technique for mapping shorelines; the vehicle can drive on a shoreline of interest with a constant speed (Morton et al. 1993). In general, this method is highly accurate, low in cost, and rapid in collecting data (Morton and Speed 1998). Boak and Turner (2005) draw attention to this approach, but they noted that error in measurement is associated with visual determination rather than with the measurements themselves, highlighting the method's accuracy over aerial imagery. However, the accuracy depends on the spatial accuracy of the GPS device.

The use of satellite images can provide high quality shoreline mapping data. However, this depends on the spatial resolution (Klemas 2010). This technique is used because of its wide area coverage, which saves time and effort, and its spectral capability of detecting differences between land and water features using infrared bands captured through the sensors, which gives it an advantage over other techniques (Alesheikh, Ghorbanali, and Nouri 2007). Some satellite image data are free, such as Landsat data, and some (high spatial resolution) are from commercial sources, such as IKONOS, Quickbird, and Worldview. To detect coastline changes accurately, high spatial resolution data are required (Klemas 2010). Such data can be expensive.

Light detection and ranging (LIDAR) is the most recent and accurate technique for mapping shorelines. This method is based on measuring the travel time of laser beam from the time it leaves the device, to its return after reflection (Cracknell 1999). It collects three-dimensional points that include an x , y , and z value. Unlike aerial photos and satellite images, LIDAR allows scientists to measure the volume change. Despite its

high cost, it covers large areas in a short time, making it the preferred method (Boak and Turner 2005).

Using Remote Sensing and GIS in Shoreline Change Detection: Methodological Considerations

Shorelines are very dynamic features and they change constantly. Thus, using remote sensing and GIS in conducting shoreline change detection is a very complex task because it consists of sequential steps, and each step could produce an error. Because these steps are sequential, errors are cumulative. Hence, methodological issues must be taken into consideration.

Spatial and Spectral Resolution of Satellite Images

The extent of the spatial area on the ground from which the measurements that comprise the remotely sensed data are acquired is known as spatial resolution (Townshend 1980). The spatial and spectral resolutions of satellite images are the first consideration. Thus, a higher level of detail and features can be acquired with the high spatial resolution of satellite images (Rocchini 2007). Hence, the larger the pixel size, the coarser the resolution, and the larger the error in identifying a shoreline's position (Del Río and Gracia 2013). This is because lower resolution satellite images are less sensitive to spatial complexity as they tend to include mixed pixel issues (Rocchini 2007). Spectral resolution is also important in shoreline change detection. Since the ultimate goal is to separate water from land, and since the high of the reflectance of water is within the green or blue wavelengths (depending on the chlorophyll level in the water) and the high reflectance of soil is in near-infrared reflectance (NIR) (Bouchahma and Yan 2012), satellite images need to have at least a four-band bundle image to be used for the

automatic shoreline extraction method. However, a natural color image is sufficient for digitizing the shoreline manually.

Geometric Correction

The efficient use of remotely sensed data in change detection is dependent not only the spatial and spectral resolutions, but also on the preprocessing procedures (Anuta et al. 1984; Townshend et al. 1992). During the process of capturing satellite images or aerial photos, these images or photos are subjected to positional distortions caused by the satellite or plane motion and the camera or sensor system (Van Wie and Stein 1976). These distortions will greatly affect the accuracy and quality of data (Rifman 1973); hence, geometric correction is needed. Geometric correction can be achieved by georeferencing the satellite image or aerial photo using polynomial transformation based on ground control points (Del Río and Gracia 2013). Ground control points can be collected either by using DGPS field survey or from another already georeferenced image or map. In either case, collecting or choosing ground control points must be done carefully (Moore 2000; Wolf and Dewitt 2000; Del Río and Gracia 2013) and must follow the general criteria of collecting an appropriate number, evenly distributed across the area, and representing stable landmarks or features that are not subject to spatial movement, such as road intersections and buildings' corners (Moore 2000; Wolf and Dewitt 2000). The georeferencing error represented by the RMSE should be 0.5 of the pixel size (Vanderstraete, Goosens, and Ghabour 2003; Adam 2010).

Shoreline Indicators

Shoreline mapping comes after the georeferencing step. However, serious considerations need to be taken into account at this step. Since shorelines represent the

edge between land and water (Pajak and Leatherman 2002), and this edge is highly dynamic because of waves and tidal variations, shoreline proxies or indicators need to be identified on the image to minimize the effects of waves and tidal variations and to produce consistency between shorelines extracted from images or aerial photos taken on different dates. (Moore 2000; Pajak and Leatherman 2002). Scientists have used several shoreline proxies such as the high water line (HWL), the wet/dry line, the vegetation line, the dune toe, the cliff toe, and the dune crest (Coyne, Fletcher, and Richmond 1999; Pajak and Leatherman 2002; Fletcher et al. 2003; Boak and Turner 2005). However, the HWL is the most used shoreline proxy (Stafford 1971; Dolan et al. 1980; Leatherman 1983; Anders and Byrnes 1991; Crowell, Leatherman, and Buckley 1991; Morton 1991; Moore 2000; Boak and Turner 2005). The wet/dry line is widely considered to be the HWL (Crowell, Douglas, and Leatherman 1997; Boak and Turner 2005), but they are different. The HWL is defined as the dark line or debris mark that was left over from the last high tide (Pajak and Leatherman 2002) and it is more stable (McBeth 1956; Shalowitz 1964) than the wet/dry line, which migrates dynamically because of the tidal cycle (Dolan et al. 1980). Crowell, Leatherman, and Buckley (1991) stated that the HWL is the best shoreline indicator because it is easily distinguished. They also stated that the position of the HWL is nearly equivalent to the position of the mean high water line (MHW) (Crowell, Leatherman, and Buckley 1991). The MHW has been used as a standard shoreline indicator, especially in recent years, because of the existence of LIDAR technology (List and Farris 1999; Stockdonf et al. 2002; Leatherman, Douglas, and LaBrecque 2003; Robertson et al. 2004; Ruggiero et al. 2005). Unlike previous indicators (proxy-based indicators), the MHW is a tidal datum-based indicator (Boak and

Turner 2005). The MHW is the average elevation of all previous high tides recorded at a specific station for a considerable time (Ruggiero and List 2009). LIDAR has the ability to create a vertically referenced shoreline indicator based on a tidal datum such as the MHW (Stockdon et al. 2002; Allan, Komar, and Priest 2003; Parker 2003; Robertson et al. 2004; Moore, Ruggiero, and List 2006). It is used as a shoreline indicator by converting the vertical position of the MHW to a land-based datum using a Digital Elevation Model created from LIDAR (Parker 2003; Hess 2005). This type of indicator has the advantage of eliminating short-term positional sensitivity due to water dynamics such as tides and waves (List, Farris, and Sullivan 2006).

Delineation of the Shoreline Indicator

Delineating the shoreline occurs after identifying the shoreline proxy. Two methods of shoreline delineation have been developed. These methods are: manual delineation and automatic delineation. Manual delineation involves the researcher digitizing the shoreline indicator manually (Ituen, Johnson, and Njoku 2014), whereas software does the automatic delineation (Hurd et al. 2006; Alves 2007; Sekovski et al. 2014). Topan, Oruç, and Jacobsen (2009), compared both delineation techniques to digitize buildings, roads, and coastline and found that manual digitizing was more efficient than automatic digitizing, but automatic digitizing was faster.

Several methods of automatic delineation have been developed: band ratio, image classification, and image segmentation. These methods are at best intermediate steps that facilitate an analyst's delineation of the shoreline. Jayson-Quashigah, Addo, and Kodzo (2013) used band ratio (band 5/band 2) to extract the wet/dry line and achieved satisfactory results. Sekovski et al. (2014) extracted the wet/dry line using supervised

(maximum likelihood) and unsupervised (ISODATA) classification techniques and found that extracting the wet/dry line using unsupervised (ISODATA) techniques had greater accuracy than using the supervised (maximum likelihood) technique. Alves (2007) compared two image segmentation techniques (pixel-based and object-based) in extracting several shoreline indicators and found that object-based segmentation was far better than the pixel-based. Pixel-based segmentation considers only spectral reflectance, whereas object-based considers texture, size, and shape, in addition to spectral reflectance (Hurd et al. 2006).

Rate of Change Statistics

There are several tools that can be used to calculate the rate of change, but the Digital Shoreline Analysis System (DSAS) and Analyzing Moving Boundaries using R (AMBUR) are the most popular tools used to calculate rate of change statistics in the GIS environment (Jackson, Alexander, and Bush 2012). Moreover, both tools use the baseline and transects, which is the primary method for quantifying shorelines changes (Thieler et al. 2009; Jackson, Alexander, and Bush 2012). Transects are cast perpendicular from the baseline at a user-specified spacing along the shoreline (Thieler et al. 2009; Jackson, Alexander, and Bush 2012). This method is efficient over regularly shaped coastlines, but less effective over meandering shorelines, which cause the transects to overlap (Arias Moran 2003). To solve this problem, AMBUR programmers have created two new transect methods (the near and the filtered transect methods) that assist in measuring the rate of change along curved shorelines (Jackson, Alexander, and Bush 2012). From my own experience, the new updated version of DSAS solves this problem, in this case by adding a topological adjustment tool which allows the user to modify and edit transects.

Although both of these use the same shoreline analysis method (baseline and transects), they differ in the style or procedure for doing so and in the number of the statistical methods. AMBUR is based on programing and coding (Jackson, Alexander, and Bush 2012), whereas DSAS is based on clicking tools and windows (Thieler et al. 2009), which makes it more user-friendly than AMBUR. DSAS provides six rate of change statistical methods, summarized in Table 1; these include Net Shoreline Movement (NSM), Shoreline Change Envelope (SCE), Least Median of Squares (LMS), End Point Rate (EPR), Linear Regression Rate (LRR), and Weighted Linear Regression Rate (WLR) (Thieler et al. 2009), while AMBUR only provides End Point Rate (EPR), Linear Regression Rate (LRR), and Weighted Linear Regression Rate (WLR) (Jackson, Alexander, and Bush 2012).

Table 1. List of the Statistical Approaches Provided by DSAS and Their Associated Definitions. These definitions were quoted directly from Thieler et al. (2009) or from Oyedotun (2014).

Net Shoreline Movement (NSM)	Reports the distance between the oldest and the youngest shorelines.
Shoreline Change Envelope (SCE)	A measure of the total change in shoreline movement considering all available shoreline positions and reporting their distances, without reference to their specific dates.
End Point Rate (EPR)	Derived by dividing the distance of shoreline movement by the time elapsed between the oldest and the youngest shoreline positions.
Linear Regression Rate (LRR)	Determines a rate-of-change statistic by fitting a least square regression to all shorelines at a specific transects.
Weighted Linear Regression Rate (WLR)	Best-fit line is placed through the points in such a way as to minimize the sum of the squared residuals.
Least Median of Squares (LMS)	The median value of the squared residuals is used instead of the mean to determine the best-fit equation for the line.

III. RESEARCH METHODS

Site and Situation

Qaruh Island (28° 49' 5"N, 48 ° 46' 35"E) is located at the southernmost part of the Kuwaiti territorial waters (Figure 2). It is the smallest coral island in Kuwait, with an area of approximately 0.1 km² (Al-Kandari 2007). The average elevation of the island is between 5 and 7 m above sea level (Al-Kandari 2007). An elliptical-shaped reef, with length and width dimensions of 1300 m and 600 m, respectively, surrounds the Island (Al-Yamani et al. 2004). Qaruh Island is uninhabited except for some coastguards. There are no facilities except an open jetty, a coastguard building, a helicopter landing area, and a telecommunication tower. It is an unvegetated island, but it is the most diverse island in Kuwaiti waters (Al-Yamani et al. 2004). It is considered to be a breeding spot for two types of sea turtles, the green turtle (*Chelonia mydas*) and the hawksbill turtle (*Eretmochelys imbricate*) (Carpenter et al. 1997; Al-Kandari 2007). Their nesting period starts at the end of May and their eggs hatch between June and November (Al-Kandari 2007). Branching colonies and table *Acropora*, which is a type of stony coral, dominate the reef flat, with sizes of 4 m in diameter for some of them, and there are huge stands of *Porites* which is another type of stony coral (Al-Yamani et al. 2004). Other species and fish exist at the depth of 15 m. In the reef slope, there are massive *Protites lutea* colonies that are hundreds of years old (Al-Yamani et al. 2004).

Physical Conditions

Kuwait is a very small country with an area of approximately 17,818 km² and elevation ranges from 0 to 300 m (Kusky and Cullen 2010). Thus, no climate variation exists within the country's borders. Therefore, Qaruh Island and Kuwait are exposed to

the same climatic conditions. Kuwait's climate is considered to be a sub-tropical climate. The climate in Kuwait is divided into two seasons: a long, hot, and humid summer, and a cold, short winter. In the winter season, the air temperature falls to almost 0°C. However, during the summer season, temperatures can reach up to 50°C. The sea temperature varies, with daily and seasonal variations from 10°C to greater than 36°C (Al-Yamani and Saburova 2011). The sea current's direction is counterclockwise, and it moves westwards along the Iranian coast and down to the east side of the Kuwaiti coastline (Al-Yamani et al. 2004). The prevailing wind is from the northwest. Occasionally, during November, the country is exposed to the southwestern wind that comes from the Sahara desert, which is extremely hot and dry (Kusky and Cullen 2010). The average annual precipitation is 106 mm (Al-Kandari 2007), and most of the limited rainfall happens suddenly and sporadically during the winter season (Kusky and Cullen 2010). According to Buynevich et al. (2007), Qaruh and the other small Kuwaiti sub-tropical islands settled on top of small isolated platforms, which are probably of aggraded perched reef origin, and their topography descends to significantly more than 20–30 m depth within 3 km of the island.

The coastal area of Kuwait is divided into three regions based on sediment movement and coastal processes (Al-Yamani and Saburova 2011). The three coastal regions are (1) the current-dominated Khor Al-Sabbiya channel (the northeast), (2) the dynamically sheltered Kuwait Bay (the central east), and (3) the wave-dominated southern coast (Al-Yamani and Saburova 2011). Qaruh Island is situated within the wave-dominated southern coast, as shown in Figure 2. It is covered by coarse sand, and there is a small area of soft sandstone rocks at the southern beach (Al-Kandari 2007).

Except for the upper beach, which is very steep, all the other sides are sandy along the south, extending to the southwestern side (Al-Kandari 2007). According to Al-Kandari (2007), deposition occurs at the northeastern and the southwestern section, while the northwestern is exposed to a high rate of erosion and the south section is experiencing a low rate of erosion. A more detailed beach profile analysis was done by Al-Kandari (2007), who divided the island's beach into four sections. Section one represented the northwestern to the northern side and it showed significant erosion, especially at the northwestern corner; hence, a sea wall was constructed in the northwestern section to protect the shoreline from the severe erosion. The severe erosion was due to several time-wave crushing processes with a height of 2 to 2.5 meters during the northwestern wind. Scattered large shell fragments and wave-cut platforms were observed in this section. Section two represented the eastern side and it showed some old marine ridges that were rich in shells and oyster, and these ridges were cut into by land drainage. Moreover, at the end of this section, some recurved spits had formed. Sediments were fine to medium in this section. Section three represented the southern side, and sand spit and sand bars were observed as evidence of the accretion process. This section had a high number of shells and sand crabs. Section four represented the western side, where accumulated large shell fragments were observed, which reflected high wave energy due to the northwestern waves (Al-Kandari 2007).

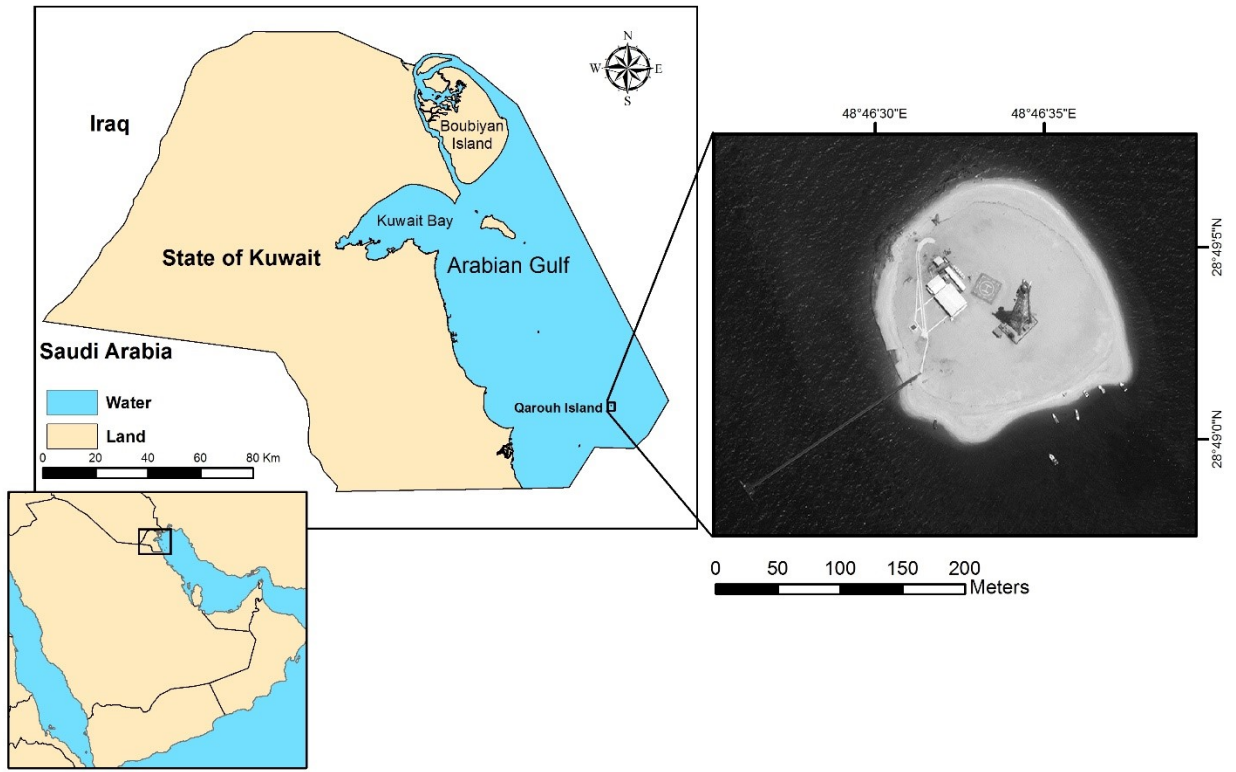


Figure 2. Map of the Study Area.

Datasets

To determine the shoreline change on Qaruh Island, I acquired two high-resolution satellite images from DigitalGlobe.com, and obtained a high waterline (HWL) survey map from the Kuwait Ministry of Municipality; each of these was from a different year: Worldview1 (2009), Worldview2 (2013), and survey map (2015). The two images are panchromatic images at 50 cm spatial resolution and the survey map was made using a 30-cm differential GPS device.

Analysis

Shoreline change detection is a very complicated process which consists of several steps. In order to get accurate results, I performed these steps in the following order:

Geometric Correction of Satellite Images

Before beginning the geometric correction process, I cropped the two images to match the extent of the study area. The geometric correction was carried out with the use of the survey map as a reference to correct the two satellite images geometrically. This type of geometric correction is called image-to-image. The first polynomial order was employed using four evenly distributed ground control points. The number of the polynomial order depends on the available number of ground control points. It can be quantified using the following equation:

$$N = \frac{(t + 1)(t + 2)}{2} \tag{1}$$

where N is the minimum number of ground control points and t is the order of the polynomial (Eltohamy and Hamza 2009). Radiometric and atmospheric corrections are not necessary because all images capture the same study area and all images are cloud-free images.

Shoreline Extraction and Calculation of Uncertainty

Shoreline extraction was carried out using manual shoreline extraction. The HWL was used as a shoreline indicator for all the images. This means that I used on-screen digitizing to digitize the HWL to create two shoreline layers (2009 and 2013). However, before digitizing the HWL, I used histogram equalization to enhance the tonal contrast for all the images. This enhanced the HWL's appearance, which led to digitizing the HWL more accurately. All extracted shoreline was saved into one feature class in the ArcMap environment. After extracting the shorelines, I used manual digitizing to draw the baseline offshore of the shorelines (Figure 3). Furthermore, to measure the rates of change, I used an ArcGIS extension called the Digital Shoreline Analysis System (DSAS). This tool computes the rates of change (erosion and accretion) alongside the extracted shorelines. DSAS requires that the attribute table of the feature class that the shorelines are saved in contains two fields. These fields are the date and the uncertainty associated with each shoreline. The uncertainty is only needed for the calculation of Weighted Linear Regression (Fletcher et al. 2012). To calculate uncertainty, Fletcher et al.'s (2012) method was used. Fletcher et al. (2012) used the following equation to calculate the uncertainty for each shoreline:

$$Ut = \pm \sqrt{Es^2 + Etd^2 + Ec^2 + Ed^2 + Ep^2 + Er^2 + Ets^2} \quad (2)$$

where E_s , E_{td} , E_c , E_d , E_p , E_r , and E_{ts} are seasonal error, tidal fluctuation error, conversion error, digitizing error, pixel error, rectification error, and T -sheet plotting error, respectively. For aerial photographs, Fletcher et al. (2012) omitted E_c and E_{ts} because they were only applicable for T -sheet. However, because I was using satellite images that were acquired within the same season (winter season), in addition to E_c and E_{ts} , I also omitted E_s . Moreover, because the HWL is the shoreline indicator that was used in this thesis (rather than the Low Water Mark, as used by Fletcher et al. (2012)), E_{td} was also omitted. Thus, to calculate the uncertainty for each extracted shoreline, the following equation was used:

$$Ut = \pm \sqrt{Ed^2 + Ep^2 + Er^2} \quad (3)$$

For the surveyed map, uncertainty was not calculated because it was not an aerial photo, satellite image, or T -sheet. In addition, it is an outside source and the only information obtained with it was the date and the accuracy. Thus, the accuracy of the surveyed map (0.30 cm) was considered as its uncertainty. Table 3 contains all error types and the calculated uncertainty for each shoreline.

Rate of Change Calculation

After calculating the uncertainty for each shoreline, I constructed transects by setting the distance between transects to 10 m. Setting the distance to 10 m provides more details than setting it to 20 or 50 m (Figure 3). In order to calculate the rate of change, I used NSM, EPR, LRR, and WLR statistical measurements. However, LRR and WLR are only applicable when using more than two shorelines. The analytic process resulted in a variety of maps that show areas of erosion and accretion with different colors for each.

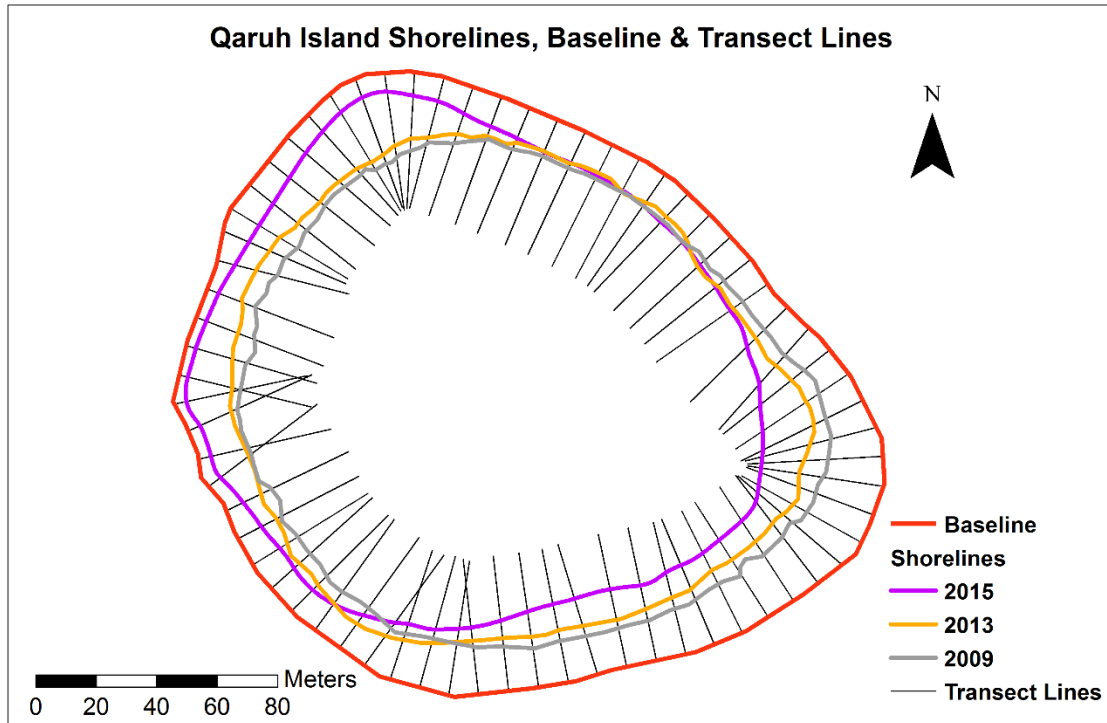


Figure 3. Map Showing the Extracted Shorelines, Baselines, and Transect Lines.

Table 2. Value of Errors and Uncertainty Associated with Each Shoreline.

Shoreline	E_d	E_p	E_r	Uncertainty
2009	0.280526 m	0.5 m	0.240095 m	± 0.621563 m
2013	0.181868742 m	0.5 m	0.228315 m	± 0.578968 m
2015	-	0.3 m	-	± 0.3 m

Fieldwork

In the last stage, and after getting the DSAS result, fieldwork was carried out in order to validate the results of the analysis results. The fieldwork was conducted on January 11, 2016, using a photo-taking approach. It was carried out during the low-tide period. I validated the final maps by surveying each section in the field. For instance, I surveyed the erosion area indicated by the map. This helped in validating the result, and in linking erosion to the factors responsible for it.

IV. RESULTS

The results of the shoreline analysis were classified into three periods (2009–2013, 2013–2015, and the overall shoreline change 2009–2015). In regard to the first two intervals (2009–2013 and 2013–2015), two rate of change methods were used (End of Points and Net Shoreline Measurement). This is because these are the only two methods that can be applied when using two shorelines. Linear Regression and Weighted Linear Regression need a minimum of three shorelines.

Shoreline Change from 2009 to 2013

Shoreline change from 2009 to 2013 is included in Figures 4 and 5. Figure 4 shows the result of the End of Point method from 2009 to 2013. In this figure, it is clear that there has been a shoreline retreat (erosion) from the east to the south part of the island. This part of the island has experienced a retreat of -2.1 – -0.4 m/y. On the other hand, accretion is occurring from the northwest to the southwest part of the island. This section was exposed to accretion of 0.8 – 1.6 m/y. Moreover, the north to the northeast part and a small portion of the west part of the island has experienced a change of -0.4 – -0.8 m/y. This rate of change quantity was classified as of the no change class because there was only slight difference in the rate of change between the two periods (2009–2013). Moreover, Figure 5 shows the result of the Net Shoreline Movement method from 2009 to 2013. In this figure, it is clear that between 2009 and 2013, the shoreline experienced a change of -8.4 – -1.7 (erosion), 3.1 – 6.5 m (accretion), -1.7 – 3.1 m (no change), in the east to the south part, the northwest to the southwest part, and the north to

the northeast part and a small portion of the west part of the island, respectively.

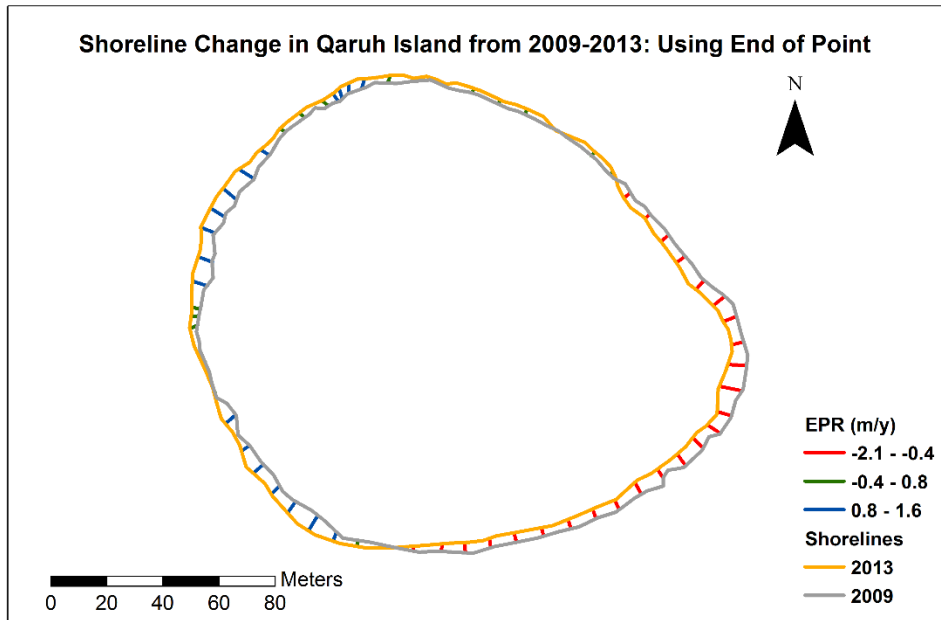


Figure 4. Map Showing the Result of the End of Point Method, 2009–2013.

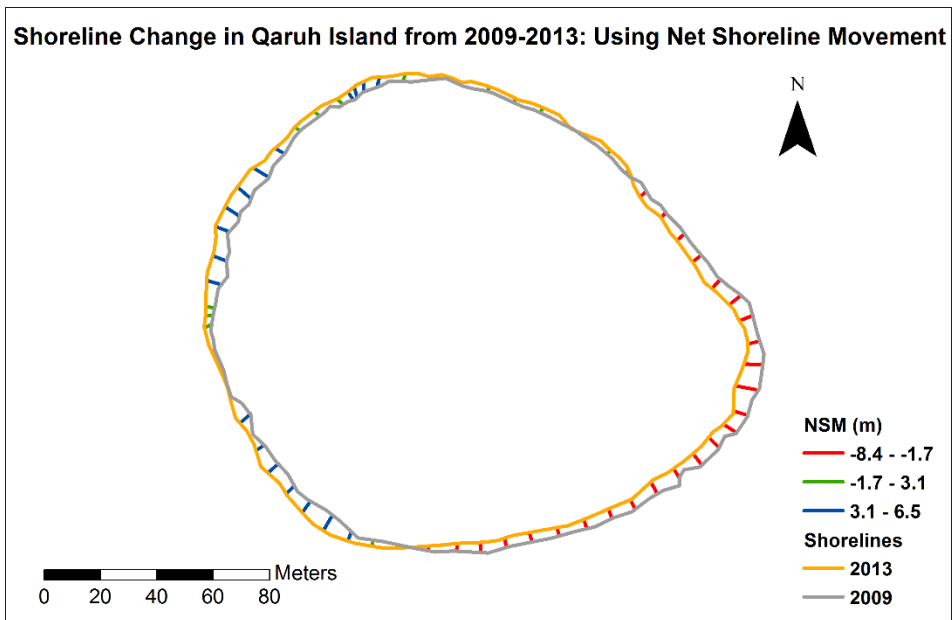


Figure 5. Map Showing the Result of the Net Shoreline Movement Method, 2009–2013.

Shoreline Change from 2013 to 2015

The result of the shoreline change analysis from 2013 to 2015 show erosion and accretion trends similar to the result of 2009 to 2013 (Figures 6 and 7). Figure 6 shows the result of the End of Point method from 2013 to 2015. In this figure, it is clear that there has been a shoreline retreat (erosion) from the east to the south part of the island. This part of the island has experienced a retreat of $-8.7 - -2.7$ m/y. In contrast, accretion is occurring from the north to the west part of the island. This section experienced to accretion of $2.68 - 10$ m/y. Moreover, the northeast part to the east part and a small portion of the southwest part of the island have experienced a change of $-2.7 - -2.68$ m/y. This rate of change quantity was classified as of the no change class because there was only a slight difference in the rate of change between the two periods (2013–2015). Furthermore, Figure 7 shows the result of the Net Shoreline Movement method from 2013 to 2015. In this figure, it is obvious that between 2013 and 2015, the shoreline experienced a change of $-17.3 - -5.4$ (erosion), $5.3 - 19.8$ m (accretion), and $-5.4 - 5.3$ (no change), in the east to the south part, the north to the east part of the island, and the northeast part and a small portion in the southwest, respectively.

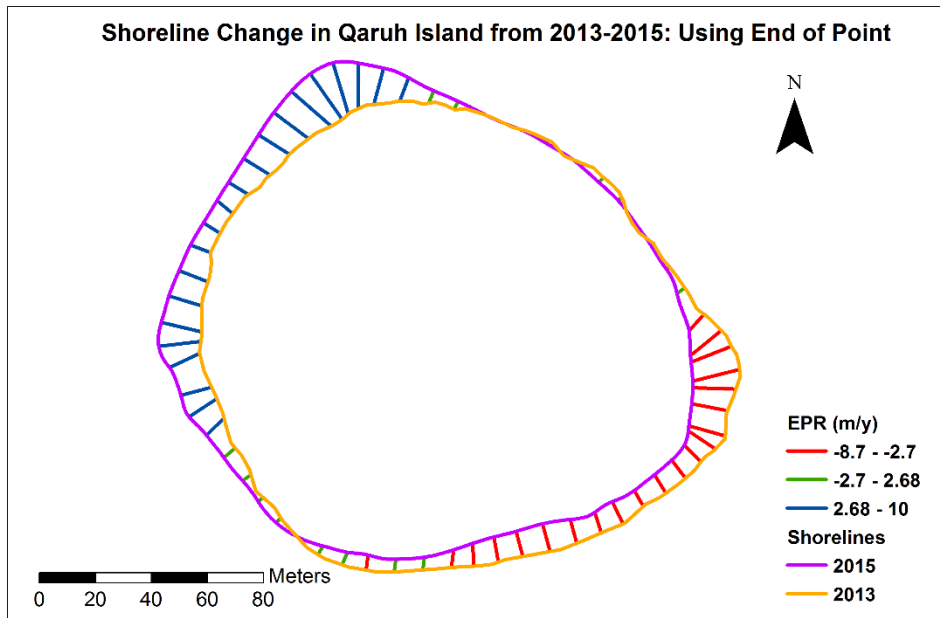


Figure 6. Map Showing the Result of the End of Point Method, 2013–2015.

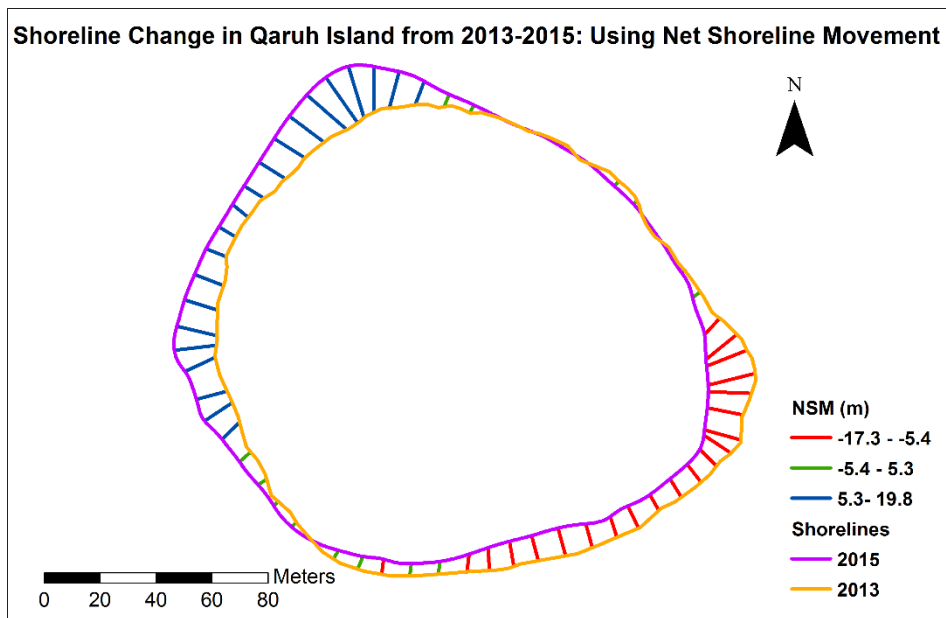


Figure 7. Map Showing the Result of the Net Shoreline Movement Method, 2013–2015.

Shoreline Change from 2009 to 2015

Shoreline change from 2009 to 2015 is shown in Figures 8 through 11. Since all rate of change methods showed the same morphodynamic trend during this period, only the result of End of Point (Figure 8) and Net Shoreline Movement (Figure 9) will be reported and the results of Linear Regression (Figure 10) and Weighted Linear Regression (Figure 11) will not be reported. Figure 8 shows the result of the End of Point method from 2009 to 2015. In this figure, it is clear that there was a shoreline retreat (erosion) from the east to the south part of the island. This part of the island experienced a retreat of $-3.7 - -1.2$ m/y. On the other hand, accretion was occurring from the north to the west part of the island. This section was exposed to accretion of $1.19 - 3.9$ m/y. Moreover, the north to the northeast part and the southwest part of the island experienced a change of $-1.2 - 1.19$ m/y. This rate of change quantity was classified as of the no change class because there was only a slight difference in the rate of change between the two periods (2009–2015). Moreover, Figure 9 shows the result of the Net Shoreline Movement method from 2009 to 2015. In this figure, it is clear that between 2009 and 2015, the shoreline experienced a change of $-8.4 - -1.7$ m (erosion), $3.1 - 6.5$ m (accretion), and $-1.7 - 3.1$ m (no change), in the east to the south part, the northwest to the southwest part, and the north to the northeast part and a small portion of the west part of the island, respectively.

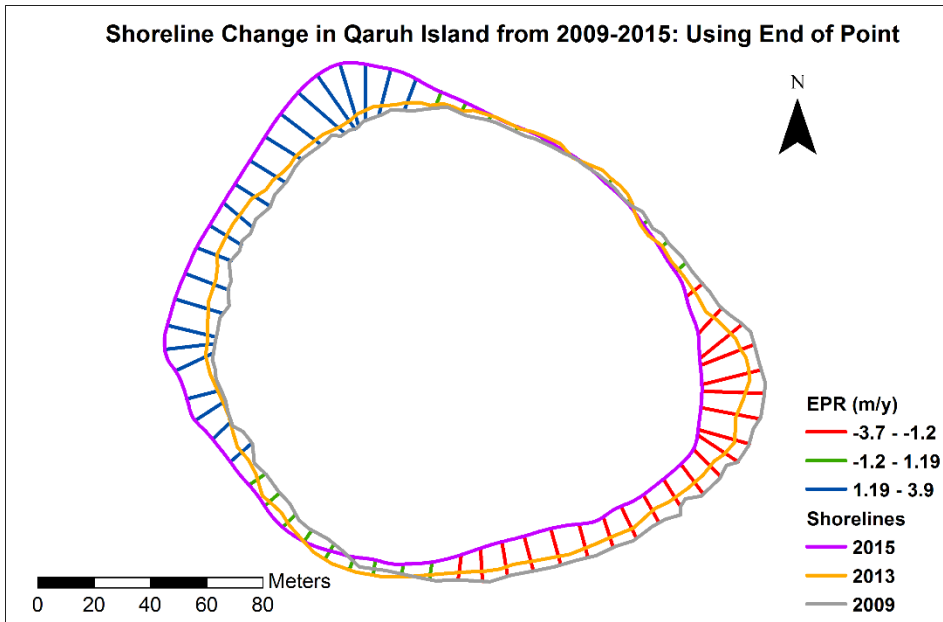


Figure 8. Map Showing the Result of the End of Point Method, 2009–2015.

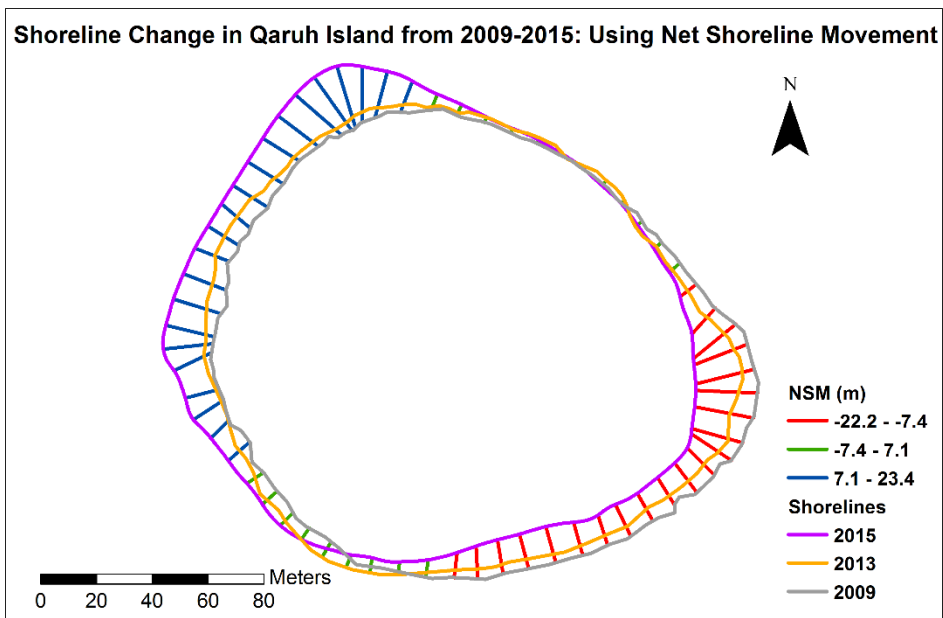


Figure 9. Map Showing the Result of the Net Shoreline Movement Method, 2009–2015.

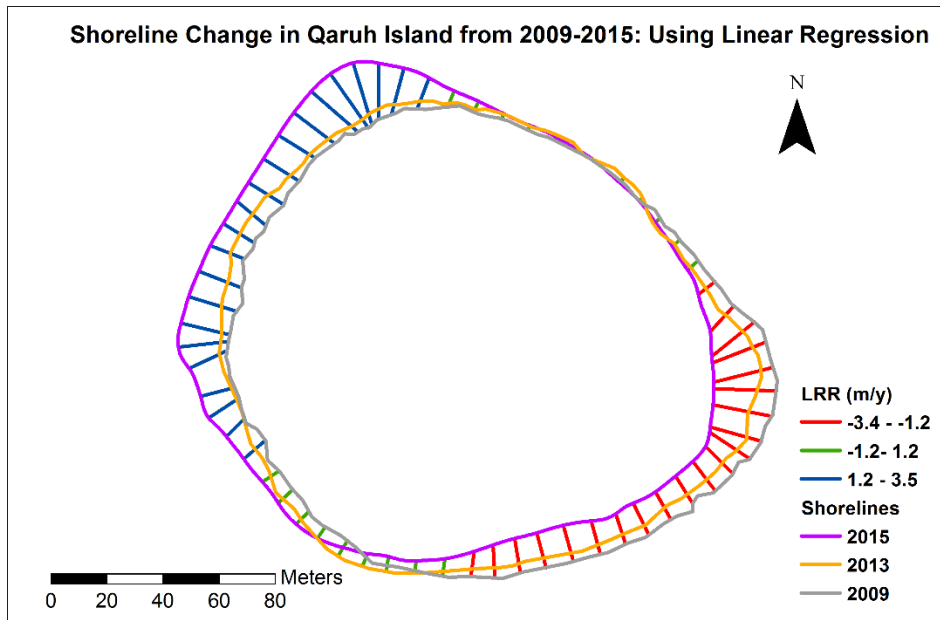


Figure 10. Map Showing the Result of the Linear Regression Method, 2009–2015.

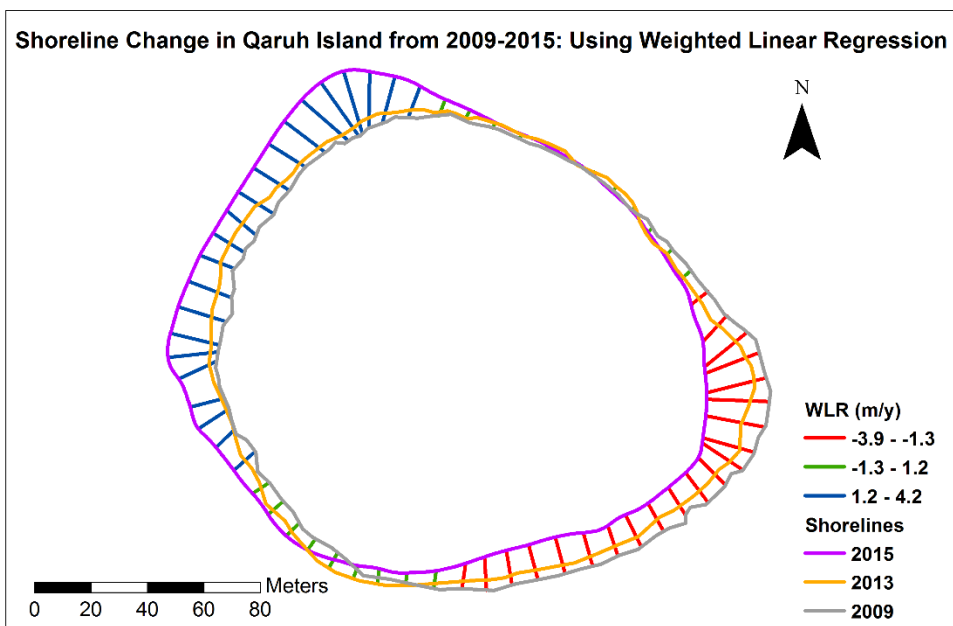


Figure 11. Map Showing the Result of the Weighted Linear Regression Method, 2009–2015.

Fieldwork Result: Shoreline Change Verification

The result of the fieldwork observation matches the DSAS tool result. In the southeast part of the island where the erosion is taking place according to the DSAS result, a 30-cm wave-cut platform was found (Figure 12). The wave-cut platform extends for approximately 43 m. In the northern to the west part of the island where the accretion is taking place according to the DSAS result, a man-made seawall was found (Figure 13). Beach ridges were found in all accretion areas (Figure 14). These beach ridges confirm that these parts of the island are experiencing accretion activities. In the southwest side of the island where the accretion is taking place according to the DSAS result, a small sand dune was found underneath the jetty and beach ridges were also found in this area (Figure 15). Moreover, in the northeast and the west part of the island where the no change class exists (erosion = accretion) according to the DSAS result, beach cusps were found. These cusps were formed as a result of eroded beach ridges (depositional landforms), which indicates that this area is experiencing depositional and erosional activities (Figure 16).



Figure 12. Photo Showing the Wave-Cut Platform in the Southeast Part of the Island.



Figure 13. Photo Showing the Seawall in the Northwest Part of the Island.



Figure 14. Photo Showing Beach Ridges in Accretion Areas.



Figure 15. Photo Showing Small Sand Dune Underneath the Jetty and Beach Ridges in the Southwest Part of the Island.



Figure 16. Photo Showing Cusps in the No Change Area.

V. DISCUSSION

It is clear that all time intervals show the same morphodynamic trend (2009–2013, 2013–2015, 2009–2015). Thus, instead of discussing each interval separately, the discussion will be mainly built on the constant morphodynamic trend that all these time intervals are experiencing. However, some explanation will be provided regarding the difference in the magnitude of change between the 2009–2013 and the 2013–2015 intervals.

It is clear that erosion extends from the east to the south part of the islands, despite the wind rose (Figure 17) and wave rose (Figure 18), which show that the prevailing wind and waves are coming from the north and the northwest. This is because the north and northwestern fetch (Figure 19) and depth (Figure 20) are much less than the fetch and depth that the southeastern wind blows over. Thus, the northwestern waves have low-energy while the southeastern waves have large-energy. In more detail, the northwestern waves (low-energy) can be considered constructive waves whose swash is bigger than their backwash (Pask, Tieh, and Pask 2007). As a result, sediments are carried onto the beach (deposition). Conversely, the southeastern waves can be considered destructive waves whose backwash is greater than their swash (Pask, Tieh, and Pask 2007). Because of destructive waves, sediment is carried away from the land (erosion). Also, the seawall that extends from the north to the west part of the island is responsible for protecting this part from erosion by mitigating the northwestern wave's energy. Beside its protective role, it is clear that the seawall is responsible for trapping the eroded sediments from the east to the south part of the island. Longshore drift is responsible for moving the eroded sediments from the east to the north and from the

southeast and the south to the west. This movement depends on the angle of the breaking waves on the shoreline. Moreover, the south part of the island, which is experiencing erosion, seems to be affected by anthropogeomorphic activities. In more detail, people can only access and park their boats on the island through the south part (Figure 21). This is because the seawall is constructed in the north to the west part, fringing reef is extremely close to the eastern part, which might cause the boats to be stacked on the reef (Figure 22), and parking boats in the jetty is only allowed for officials such as coast guards. Parking and pulling out boats in this part of the island is inducing erosion. Specifically, in the parking stage, the heavy weight of the boat will make the sand more cohesive and smash the crust of the soil. In the pulling out stage, sand will be pulled out from the land to the water.

In regard to the no change class in the north east and south west parts, the wind rose and wave rose show that these parts of the island are not exposed to effective winds and waves (Figures 17 and 18). Furthermore, it is obvious that the rate of change between the 2009–2013 period and the 2013–2015 period almost doubled during half of the total time period. This might be due to using the survey map, which is an outside source about which no further information rather than its date and accuracy is known (see the Conclusion chapter).

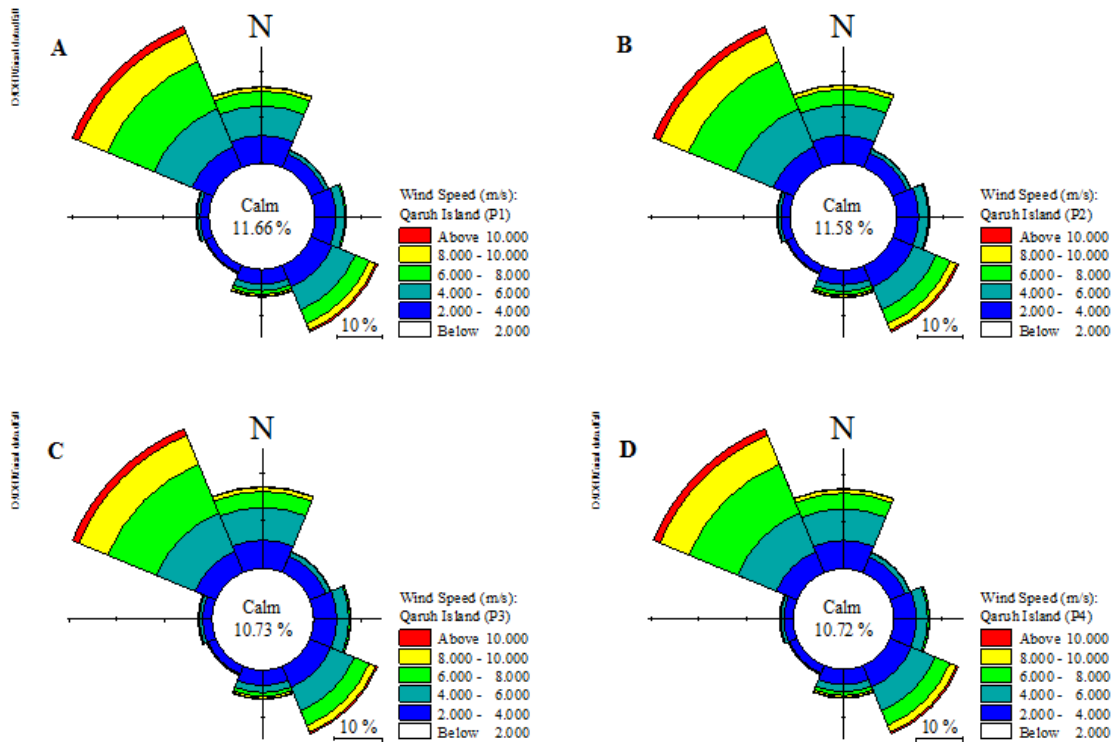


Figure 17. Wind Rose around Qaruh Island. Each wind rose represent a location near Qaruh island (A represents a location north west of the island, B north east, C south west, and D south east) (Mohamad Alkhalidi, Assistant Professor of Coastal & Ocean Engineering, Kuwait University, January 4, 2016, e-mail message to author).

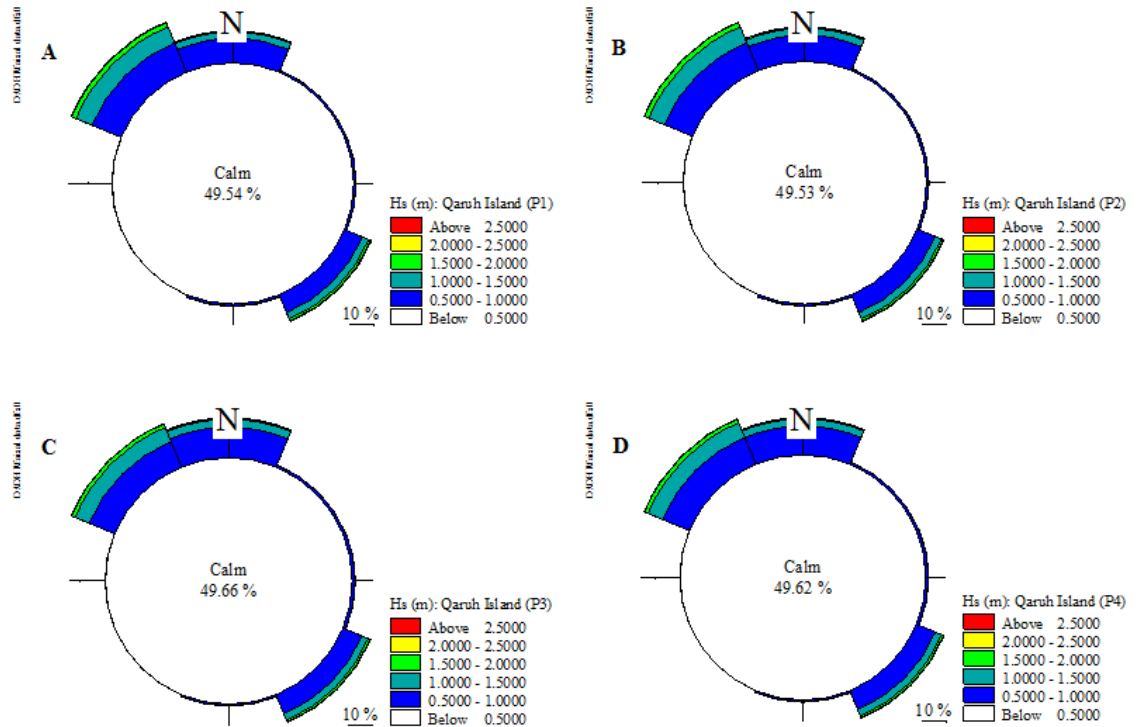


Figure 18. Wave Rose around Qaruh Island. Each wave rose represents a location near Qaruh island (A represents a location north west of the island, B north east, C south west, and D south east) (Mohamad Alkhalidi, Assistant Professor of Coastal & Ocean Engineering, Kuwait University, January 4, 2016, e-mail message to author).



Figure 19. Nautical Chart of the Arabian Gulf with Red Circle Showing Qaruh's Location (Mohamad Alkhalidi, Assistant Professor of Coastal & Ocean Engineering, Kuwait University, January 4, 2016, e-mail message to author).

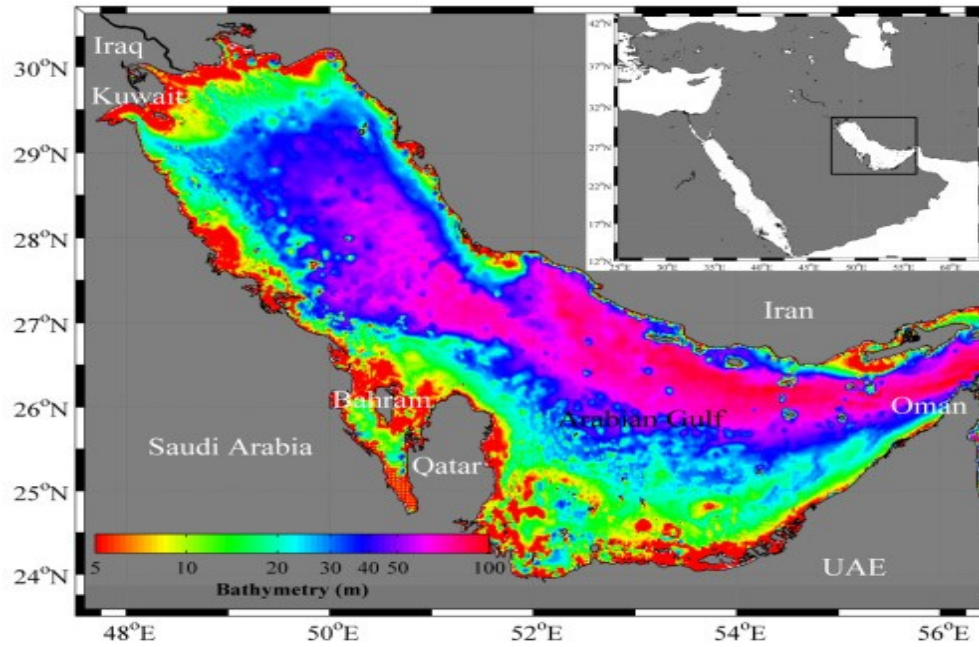


Figure 20. Bathymetry Map of the Arabian Gulf (Zhao et al. 2014).



Figure 21. Satellite Image of the Study Areas Showing the Location of Boats on the Island.



Figure 22. Aerial Photo of the Island Showing How Closely the East Part Is Fringed by the Reef (Mohamad Alkhalidi, Assistant Professor of Coastal & Ocean Engineering, Kuwait University, January 4, 2016, e-mail message to author).

VI. CONCLUSION

The shorelines of coral islands are hypothesized to be constantly changing—changed directly by waves, longshore drift, tides, and anthropogenic activities, and indirectly by factors affecting the coral reef that surrounds the shorelines. Since these islands are ecologically important, many scientists have been evaluating this change to understand it and mitigate it. Scientists have used several methods, including GPS, aerial photography, LIDAR, and remote sensing, to assess short-term and long-term shoreline change. Qaruh Island is a Kuwaiti coral island that is the most diverse area in Kuwait's water territory, and it is facing severe shoreline change. To understand the situation, I carried out an in-depth study to detect the magnitude and direction of the shoreline change with the aim of determining the natural and the anthropogenic factors responsible for the change in the Qaruh shoreline. The questions that this research has answered are as follows: (i) How did the shoreline of Qaruh Island off the shore of Kuwait change from 2009 to 2015? (ii) What is the magnitude, direction, and change rate of the shoreline of Qaruh Island? The Digital Shoreline Analysis System was applied to investigate the magnitude and trend between three extracted shorelines, each of which represented a different year. Two of the extracted shorelines were extracted from Worldview1 (2009) and Worldview2 (2013). The results of this research are different than those of previous studies on the same site by Al-Kandari (2007) and Neelamani et al. (2007). This might be because Al-Kandari (2007) used wave climate data that came from a study conducted in 1989. This means that the result of Al-Kandari (2007) did not take into consideration the existence of the seawall. Moreover, Al-Kandari (2007) used low-resolution bathymetry data, which affects the quality of the result. Moreover, the result of the shoreline change

analysis conducted by Neelamani et al. (2007) was based on Landsat satellite images, which are very coarse compared to the data that I used. The result of this thesis shows that Qaruh Island is experiencing a severe erosion in the east to the south part of its shoreline and a severe accretion in the north to the west part of the island. However, since the island is experiencing approximately the same amount of erosion and accretion, this is evidence that the island is experiencing a natural process. Thus, I conclude that the island is in a normal condition and hard structures are not needed. However, this thesis has some limitations, which are as follows: (i) Different types of data were used in this thesis (two satellite images and a survey map) due to the unavailability of a third satellite image within the winter season. Using the survey map alongside the satellite images represents an inconsistency in the analysis. This is because the HWL in the survey map was delineated in the field where it is affected by human errors and the wave conditions of the day on which it was delineated. In contrast, the HWL in the satellite images were digitized manually by the same person. Furthermore, the survey map is an outside data source about which a great deal of information is unknown, such as how they surveyed the HWL. (ii) Satellite images were used because of the unavailability of LIDAR and shoreline GPS. Thus, the magnitude of change will be represented in (m), which represents distance, instead of volume (m^3). This is due to the absence of high-resolution topographic data which can be constructed by using LIDAR. (iii) Future shoreline predictions were not established because the only available data are considered to be on a short-term temporal scale, which is not enough for predictions about the future.

To overcome these limitations, I offer the following recommendations:

- 1- Future studies need to concentrate on using the LIDAR technique, which allows for doing tidal-based shoreline change analysis, provides consistency, and allows for the quantification of shoreline change in volume (m^3) instead of distance (m).
- 2- Future studies should conduct comparative seasonal shoreline change detection, which will allow the Kuwaiti government to know the status of the island seasonally.
- 3- The Kuwaiti government needs to make the needed data accessible to scholars, which will encourage scholars to conduct research on the State of Kuwait.

REFERENCES

- Adam, H. E. 2010. Integration of remote sensing and GIS in studying vegetation trends and conditions in the Gum Arabic Belt in North Kordofan, Sudan. Dissertation, Technische Universität Dresden.
- Allan, J. C., P. D. Komar, and G. R. Priest. 2003. Shoreline variability on the high-energy Oregon coast and its usefulness in erosion-hazard assessments. *Journal of Coastal Research* Special Issue 38: 83-105.
- Alesheikh, A. A., A. Ghorbanali, and N. Nouri. 2007. Coastline change detection using remote sensing. *International Journal of Environmental Science & Technology* 4 (1): 61-66.
- Al-Kandari, S. 2007. Development of environmental impact assessment (EIA) Procedures for the sustainability of small islands: A case study, State of Kuwait. Master's thesis, Department of Environmental Science, Kuwait University.
- Al-Yamani, F. Y., J. Bishop, E. Ramadan, M. Al-Husaini, and A. N. Al-Ghadban. 2004. *Oceanographic atlas of Kuwaiti waters*. Safat, Kuwait: Kuwait Institute for Scientific Research.
- Al-Yamani, F. Y., and Saburova, M. A. 2011. *Illustrated guide on the benthic diatoms of Kuwait's marine environment*. Safat, Kuwait: Kuwait Institute for Scientific Research.
- Alves, M. V. M. 2007. Detection of physical shoreline indicators in a[n] object-based classification approach. Thesis, International Institute for Geo-Information Science and Earth Observation, Enschede: The Netherlands.
- Anders, F. J., and M. R. Byrnes. 1991. Accuracy of shoreline change rates as determined from maps and aerial photographs. *Shore and Beach* 59 (1): 17-26.
- Anuta, P. E., L. A. Bartolucci, M. E. Dean, D. F. Lozano, E. Malaret, C. D. McGillem, J. A. Valdes, and C. R. Valenzuela. 1984. LANDSAT-4 MSS and Thematic Mapper data quality and information content analysis. *IEEE Transactions on Geoscience and Remote Sensing* GE-22 (3): 222-36.
- Arias Moran, C. A. 2003. Spatio-temporal analysis of Texas shoreline changes using GIS technique. Master's thesis, Texas A&M University.
- Barnes, R. D. 1987. *Invertebrate zoology*, 5th ed. Fort Worth, TX: Harcourt Brace Jovanovich College Publishers.
- Bellwood, D. R. 1995. Carbonate transport and within-reef patterns of bioerosion and sediment release by parrotfishes (family Scaridae) on the Great Barrier Reef. *Marine ecology progress series. Oldendorf* 117 (1): 127-36.

- Block, H. [2007]. Coral reef zonation.
<http://www.unc.edu/courses/2007fall/masc/490/001/Coral%20Reef%20Decline/Zonation.html> (last accessed 21 October 2015).
- Boak, E. H., and I. L. Turner. 2005. Shoreline definition and detection: A review. *Journal of Coastal Research* 21 (4): 688-703.
- Bouchahma, M., and W. Yan. 2012. Automatic measurement of shoreline change on Djerba Island of Tunisia. *Computer and Information Science* 5 (5): 17-24.
- Butler, D. R. 1995. *Zoogeomorphology: Animals as geomorphic agents*. Cambridge, UK: Cambridge University Press.
- Buynevich, I. V., D. M. Fitzgerald, A. Al-Zamel, and M. Al-Sarawi. 2007. Geomorphology and sedimentary framework of small subtropical islands, offshore Kuwait. Paper presented at the 2007 GSA Denver Annual Meeting, Denver, CO.
- Carpenter, K. E., P. L. Harrison, G. Hodgson, A. H. Alsaffar, and S. H. Alhazeem. 1997. *The corals and coral reef fishes of Kuwait*. Safat, Kuwait: Kuwait Institute for Scientific Research.
- Carté, B. K. 1996. Biomedical potential of marine natural products. *BioScience* 46 (4): 271-86.
- Coyne, M. A., C. Fletcher, and B. Richmond. 1999. Mapping coastal erosion hazard areas in Hawaii: Observations and errors. *Journal of Coastal Research* Special issue 28: 171-84.
- Cracknell, A. 1999. Remote sensing techniques in estuaries and coastal zones an update. *International Journal of Remote Sensing* 20 (3): 485-96.
- Crowell, M., S. P. Leatherman, and M. K. Buckley. 1991. Historical shoreline change: error analysis and mapping accuracy. *Journal of Coastal Research* 7 (3): 839-52.
- Crowell, M., B. C. Douglas, and S. P. Leatherman. 1997. On forecasting future US shoreline positions: A test of algorithms. *Journal of Coastal Research* 13 (4): 1245-55.
- Darwin, C., and T. G. Bonney. 1897. *The structure and distribution of coral reefs*. New York: D. Appleton.
- Davidson-Arnott, R. 2010. *Introduction to coastal processes and geomorphology*. Cambridge, UK: Cambridge University Press.
- Del Río, L., and F. J. Gracia. 2013. Error determination in the photogrammetric assessment of shoreline changes. *Natural Hazards* 65 (3): 2385-97.

- Dimitrov, R. 2006. *Science and International environmental policy: Regimes and nonregimes in global governance*. Lanham, MD: Rowman & Littlefield.
- Dodge, R. E., and T. R. Gilbert. 1984. Chronology of lead pollution contained in banded coral skeletons. *Marine Biology* 82 (1): 9-13.
- Dolan, R., B. P. Hayden, P. May, and S. May. 1980. The reliability of shoreline change measurements from aerial photographs. *Shore and Beach* 48 (4): 22-29.
- Eltohamy, F., and E. Hamza. 2009. Effect of ground control points location and distribution on geometric correction accuracy of remote sensing satellite images. Paper presented at the 13th International Conference on Aerospace Sciences & Aviation Technology, ASAT-13, May 26-28, 2009, Cairo, Egypt.
- Fletcher, C., J. Rooney, M. Barbee, S.-C. Lim, and B. Richmond. 2003. Mapping shoreline change using digital orthophotogrammetry on Maui, Hawaii. *Journal of Coastal Research* Special Issue 38: 106-124.
- Fletcher, C. H., B. M. Romine, A. S. Genz, M. M. Barbee, M. Dyer, T. R. Anderson, S. C. Lim, S. Vitousek, C. Bochicchio, and B. M. Richmond. 2012. *National assessment of shoreline change: Historical shoreline change in the Hawaiian Islands*. U.S. Department of the Interior, Open-File Report 2011-1051. Reston, VA: U.S. Geological Survey.
- Galko, F. 2002. *Coral reef animals*. Chicago: Heinemann Library.
- Goldberg, W. M. 2013. *The biology of reefs and reef organisms*. Chicago: University of Chicago Press.
- Goudie, A. S., and H. A. Viles. 2013. *The earth transformed: An introduction to human impacts on the environment*. Oxford: Wiley.
- Graham, D., M. Sault, and C. J. Bailey. 2003. National ocean service shoreline—past, present, and future. *Journal of Coastal Research* Special Issue 38: 14-32.
- Hallock, P. 1988. The role of nutrient availability in bioerosion: Consequences to carbonate buildups. *Palaeogeography, Palaeoclimatology, Palaeoecology* 63 (1-3): 275-91.
- Hess, K. W., E. Spargo, A. Wong, S. A. White, and S. K. Gill. 2005. *VDatum for central coastal North Carolina: Tidal datums, marine grids, and sea surface topography*. NOAA Technical Report NOS CS 21. Silver Spring, MD: U.S. Department of Commerce, National Oceanic and Atmospheric Administration, National Ocean Service, Office of Coast Survey, Coast Survey Development Laboratory.
- Houston, J. R. 2015. Shoreline Response to sea-level rise on the southwest coast of Florida. *Journal of Coastal Research* 31 (4): 777-89.

- Houston, J. R., and R. G. Dean. 2014. Shoreline change on the east coast of Florida. *Journal of Coastal Research* 30 (4): 647-60.
- Howard, L. S., and B. E. Brown. 1984. Heavy metals and reef corals. *Oceanography and Marine Biology Annual Review* 22: 195-210.
- Huggett, R. 2011. *Fundamentals of Geomorphology*. London: Taylor & Francis.
- Hurd, J. D., D. L. Civco, M. S. Gilmore, S. Prisloe, and E. H. Wilson. 2006. Tidal wetland classification from Landsat imagery using an integrated pixel-based and object-based classification approach. Paper presented at the American Society for Photogrammetry and Remote Sensing, 2006 Annual Conference, Reno, NV.
- Hutchings, P. 2010. Bioerosion. In *Encyclopedia of modern coral reefs: Structure, form, and process*, ed. D. Hopley, 139-55. Encyclopedia of Earth Sciences series. Dordrecht, The Netherlands: Springer.
- Ituen, U. J., I. U. Johnson, and J. C. Njoku. 2014. Shoreline change detection in the Niger Delta: A case study of Ibeno shoreline in Akwa Ibom State, Nigeria. *Global Journal of Human-Social Science Research* 14 (6): 25-34.
- Jackson, C. W., Jr., C. R. Alexander, and D. M. Bush. 2012. Application of the AMBUR R package for spatio-temporal analysis of shoreline change: Jekyll Island, Georgia, USA. *Computers & Geosciences* 41: 199-207.
- Jayson-Quashigah, P.-N., K. A. Addo, and K. S. Kodzo. 2013. Medium resolution satellite imagery as a tool for monitoring shoreline change. Case study of the eastern coast of Ghana. *Journal of Coastal Research* Special Issue 65: 511-16.
- Karleskint, G., R. Turner, and J. Small. 2012. *Introduction to marine biology*. Belmont, CA: Brooks/Cole, Cengage Learning.
- Karlson, R. H. 2002. *Dynamics of coral communities*. Dordrecht, The Netherlands: Kluwer Academic Publishers.
- Kato, A. 2008. *Capturing tree crown attributes from high resolution remotely sensed data*. Dissertation, University of Washington.
- Keller, E. A., and D. E. DeVecchio. 2011. *Natural hazards: Earth's processes as hazards, disasters, and catastrophes*. Upper Saddle River, NJ: Pearson Education, Pearson Prentice Hall.
- Klemas, V. 2010. Remote sensing techniques for studying coastal ecosystems: An overview. *Journal of Coastal Research* 27 (1): 2-17.
- Kusky, T. M., and K. E. Cullen. 2010. *Encyclopedia of earth and space science* (2 vols). New York: Facts on File.

- Lalli, C.M., and T.R. Parsons. 1995. *Biological oceanography: An introduction*. Oxford,: Butterworth-Heinemann Ltd.
- Leatherman, S. P. 1983. Shoreline mapping: A comparison of techniques. *Shore and Beach* 51 (3): 28-33.
- Leatherman, S. P., B. C. Douglas, and J. L. LaBrecque. 2003. Sea level and coastal erosion require large-scale monitoring. *Eos, Transactions American Geophysical Union* 84 (2): 13-16.
- List, J. H., and A. S. Farris. 1999. Large-scale shoreline response to storms and fair weather. In *Coastal Sediments '99*, 1324-38. Reston, VA: American Society of Civil Engineers.
- List, J. H., A. S. Farris, and C. Sullivan. 2006. Reversing storm hotspots on sandy beaches: spatial and temporal characteristics. *Marine Geology* 226 (3): 261-79.
- Liu, H. 2009. Shoreline mapping and coastal change studies using remote sensing imagery and LIDAR data. In *Remote sensing and geospatial technologies for coastal ecosystem assessment and management*, ed. X. Yang, 297-322. Berlin: Springer-Verlag.
- McBeth, F.H. 1956. A method of shoreline delineation. *Photogrammetric Engineering*, 22 (2): 400-05.
- Moberg, F., and C. Folke. 1999. Ecological goods and services of coral reef ecosystems. *Ecological Economics* 29 (2): 215-33.
- Moore, L. J. 2000. Shoreline mapping techniques. *Journal of Coastal Research* 16 (1): 111-24.
- Moore, L. J., P. Ruggiero, and J. H. List. 2006. Comparing mean high water and high water line shorelines: Should proxy-datum offsets be incorporated into shoreline change analysis? *Journal of Coastal Research* 22 (4): 894-905.
- Morgan. G. 1988. *Feasibility study on the designation of marine parks in Kuwait*. Safat, Kuwait: Kuwait Institute of Scientific Research.
- Morton, R. A. 1977. Historical shoreline changes and their causes, Texas Gulf Coast (1). *Gulf Coast Association of Geological Societies Transactions* 27: 352-64.
- . 1979. Temporal and spatial variations in shoreline changes and their implications, examples from the Texas Gulf Coast. *Journal of Sedimentary Research* 49 (4): 1101-11.
- . 1991. Accurate shoreline mapping: Past, present, and future. In *Coastal Sediments '91*, vol. 1, 997-1010. American Society of Civil Engineers.

- Morton, R. A., M. P. Leach, J. G. Paine, and M. A. Cardoza. 1993. Monitoring beach changes using GPS surveying techniques. *Journal of Coastal Research* 9 (3): 702-70.
- Morton, R. A., and F. M. Speed. 1998. Evaluation of shorelines and legal boundaries controlled by water levels on sandy beaches. *Journal of Coastal Research* 12 (4): 1373-84.
- Naylor, L. A., and H. A. Viles. 2002. A new technique for evaluating short-term rates of coastal bioerosion and bioprotection. *Geomorphology* 47 (1): 31-44.
- Naylor, L., H. Viles, and N. Carter. 2002. Biogeomorphology revisited: Looking towards the future. *Geomorphology* 47 (1): 3-14.
- Neelamani, S., U. Saif, K. Rakha, Y. Zhao, K. Al-Salem, W. Al-Nassar, A. Al-Othman, and A. Al-Ragum. 2007. Coastline Evolution of Kuwait Using Remote Sensing Techniques, EC022C. Final Report, KISR 9051, December 2007. Safat, Kuwait: Kuwait Institute for Scientific Research.
- Neteler, M., and H. Mitasova. 2002. *Open source GIS: A GRASS GIS approach*. Boston: Kluwer Academic Publishers.
- Neumann, A. C. 1966. Observations on coastal erosion in Bermuda and measurements of the boring rate of the sponge, *Cliona Lampa* 1,2. *Limnology and Oceanography* 11 (1): 92-108.
- NOAA (National Oceanic and Atmospheric Administration). 2006. 2-minute gridded global relief data (ETOPO2v2). <http://www.ngdc.noaa.gov/mgg/global/etopo2faq.html> (last accessed 27 October 2015).
- . 2014. Aerial Photography and Shoreline Mapping. <http://oceanservice.noaa.gov/geodesy/aerialphotos/> (last accessed 21 October 2015).
- Nyström, M., C. Folke, and F. Moberg. 2000. Coral reef disturbance and resilience in a human-dominated environment. *Trends in Ecology & Evolution* 15 (10): 413-17.
- Oyedotun, T. D. 2014. Shoreline geometry: DSAS as a tool for historical trend analysis. In *Geomorphological Techniques* (online edition), ed. L. E. Clarke, Chap. 3, Sec. 2.2. London: British Society for Geomorphology.
- Pajak, M. J., and S. Leatherman. 2002. The high water line as shoreline indicator. *Journal of Coastal Research* 18 (2): 329-37.
- Parker, B. B. 2003. The difficulties in measuring a consistently defined shoreline—the problem of vertical referencing. *Journal of Coastal Research* Special Issue 38: 44-56.

- Pask, T., P. Tieh, and R. Pask. 2007. *Eye for Geography Elective S3/4/5 TB S/E*. Singapore: Pearson Education South Asia.
- Reusser, L., P. Bierman, and D. Rood. 2015. Quantifying human impacts on rates of erosion and sediment transport at a landscape scale. *Geology* 43 (2): 171-74.
- Rifman, S. S. 1973. Digital rectification of ERTS multispectral imagery. *Proceedings of the Symposium on Significant Results Obtained from ERTS-1*, Vol. I, Section B, NASA SP-327, 1131–1142.
- Robertson, W., D. Whitman, K. Zhang, and S. P. Leatherman. 2004. Mapping shoreline position using airborne laser altimetry. *Journal of Coastal Research* 20 (3): 884-92.
- Rocchini, D. 2007. Effects of spatial and spectral resolution in estimating ecosystem α -diversity by satellite imagery. *Remote Sensing of Environment* 111 (4): 423-34.
- Ruggiero, P., G. M. Kaminsky, G. Gelfenbaum, and B. Voigt. 2005. Seasonal to interannual morphodynamics along a high-energy dissipative littoral cell. *Journal of Coastal Research* 21 (3): 553-78.
- Ruggiero, P., and J. H. List. 2009. Improving accuracy and statistical reliability of shoreline position and change rate estimates. *Journal of Coastal Research* 25 (5): 1069-81.
- Sekovski, I., F. Stecchi, F. Mancini, and L. Del Rio. 2014. Image classification methods applied to shoreline extraction on very high-resolution multispectral imagery. *International Journal of Remote Sensing* 35 (10): 3556-78.
- Shalowitz, A. L. 1964. *Shore and sea boundaries with special reference to the interpretation and use of coast and geodetic survey data* (Publication 10-1). Washington, DC: U.S. Government Printing Office, U.S. Department of Commerce, Coast and Geodetic Survey.
- Short, A. 2012. Coastal processes and beaches. *Nature Education Knowledge* 3 (10): 15.
- Smith, J. T. Jr. 1981. *A history of flying and photography in the Photogrammetry Division of the National Ocean Survey, 1919–79*. National Oceanic and Atmospheric Administration, National Ocean Survey. Washington, DC: U.S. Department of Commerce.
- Sorokin, Y. I. 2013. *Coral reef ecology*. Berlin: Springer.
- Spalding, M., C. Ravilious, and E. P. Green. 2001. *World atlas of coral reefs*. Berkeley: University of California Press.

- Stafford, D. B. 1971. An aerial photographic technique for beach erosion surveys in North Carolina: DTIC Document. Washington, DC: Army Coastal Engineering Research Center.
- Stockdon, H. F., A. H. Sallenger Jr., J. H. List, and R. A. Holman. 2002. Estimation of shoreline position and change using airborne topographic lidar data. *Journal of Coastal Research* 18 (3): 502-13.
- Sukcharoenpong, A. 2014. Shoreline mapping with Integrated HSI-DEM using Active Contour Method. Dissertation, Ohio State University.
- Sumich, J. L. 1996. *An introduction to the biology of marine life*, 6th ed. Dubuque, IA: Wm. C. Brown.
- Summerfield, M. A. 2014. *Global Geomorphology*. London: Routledge.
- Thieler, E. R., E. A. Himmelstoss, J. L. Zichichi, and A. Ergul. 2009. Digital Shoreline Analysis System (DSAS) version 4.0 — An ArcGIS extension for calculating shoreline change. U.S. Geological Survey Open-File Report 2008-1278. *current version 4.3.
- Topan, H., M. Oruç, and K. Jacobsen. 2009. Potential of manual and automatic feature extraction from high resolution space images in mountainous urban areas. In *ISPRS Hannover Workshop 2009: High-Resolution Earth Imaging for Geospatial Information*, 2–5 June 2009, Hannover, Germany.
- Townshend, J. R. 1980. *The spatial resolving power of earth resources satellites: A review*. September 1980. Greenbelt, MD: National Aeronautics and Space Administration, Goddard Space Flight Center.
- Townshend, J. R. G., C. O. Justice, C. Gurney, and J. McManus. 1992. The impact of misregistration on change detection. *IEEE Transactions on Geoscience and Remote Sensing* 30 (5): 1054-60.
- Tunnell, J. W., E. A. Chávez, and K. Withers. 2007. *Coral reefs of the southern Gulf of Mexico*. College Station, TX: Texas A&M University Press.
- Van Wie, P., and M. Stein. 1976. A Landsat digital image rectification system. Greenbelt, MD: Goddard Space Flight Center.
- Vanderstraete, T., R. Goosens, and T. K. Ghabour. 2003. Remote sensing as a tool for bathymetric mapping of coral reefs in the Red Sea (Hurghada—Egypt). *Belgeo* 3: 257-67.
- Vitousek, P. M., H. A. Mooney, J. Lubchenco, and J. M. Melillo. 1997. Human domination of Earth's ecosystems. *Science* 277: 494-99.

Wolf, P. R., and B. A. Dewitt. 2000. *Elements of photogrammetry with applications in GIS*. New York: McGraw-Hill.

Zhao, J., M. Temimi, H. Ghedira, and C. Hu. 2014. Exploring the potential of optical remote sensing for oil spill detection in shallow coastal waters—A case study in the Arabian Gulf. *Optics Express* 22: 13755-72.

ARABIC REFERENCES

Alsulaimani, G. 2013. Jamiat hemayat elbeaa tarod ala freeq elkhos: jazirat qaruh fe khatar. *Jaridat Alrai*. Kuwait. 9 October 2013.
<http://www.alraimedia.com/ar/article/local/2013/10/09/458417/nr/nc> (last accessed 28 October 2015).